UCRL 7322

University of California

Ernest O. Lawrence
Radiation Laboratory

CALCULATION OF ELASTIC-PLASTIC FLOW

Livermore, California

UCRL-7322
Physics, UC-34
TID-4500 (22nd Ed.)

UNIVERSITY OF CALIFORNIA
Lawrence Radiation Laboratory
Livermore, California

Contract No. W-7405-eng-48

CALCULATION OF ELASTIC-PLASTIC FLOW

Mark L. Wilkins

April 19, 1963

Printed in USA. Price $1.50. Available from the
Office of Technical Services
U. S. Department of Commerce
Washington 25, D.C.

CALCULATION OF ELASTIC-PLASTIC FLOW

Mark L. Wilkins

Lawrence Radiation Laboratory, University of California
Livermore, California

April 19, 1963

INTRODUCTION

The first requirement in the calculation of elastic-plastic flow is a formulation of the equation of state. The equation of state must describe elastic, elastic-plastic, and hydrodynamic flow. The appropriate yield criteria must be included in the latter two regimes. The literature includes many complicated forms of equations of state, some of which have been developed to aid the mathematics in the analytic solution of the equations of motion. However, since numerical techniques will be considered here, the equations of motion are completely independent of any rheological equation of state and any form may be used. The object of the equation of state will be to provide a theoretical description applicable to a wide class of practical problems, but using simple idealizations of the outstanding features of the real phenomenon.

The problems of greatest present interest pertain to metal plasticity, but detailed description of rate-dependent processes, for example, are still not well enough defined experimentally. Therefore, the plastic state will be described by continuously adjusting the stresses such that the yield strength of the material is not exceeded. More sophisticated descriptions may be included as they seem indicated by experiment.

This article is arranged in three parts: Part I – Equation of State, Part II – One-Dimensional Elastic-Plastic Flow, and Part III – Two-Dimensional Elastic-Plastic Flow.

PART I. EQUATIONS OF STATE

A. Elastic Region

We are only considering media which have the same material properties in all directions (isotropic media).

In x, y, z coordinates the state of stress in a continuous media is defined at a given point by six stress components, σ_x, σ_y, σ_z, τ_{yz}, τ_{zx}, and τ_{xy} (Ref. 1, p. 14). It is always possible to choose coordinate axes such that the shear stresses at a given point are zero i. e., such that $\tau_{yz} = \tau_{zx} = \tau_{xy} = 0$ (Ref. 2, p. 215). Any three orthogonal axes such that the above condition results are called principal axes for the point considered. The stresses in the directions of the principal axes on surfaces normal to these axes are called principal stresses, denoted by σ_1, σ_2, and σ_3.

A perfectly elastic material is characterized by a linear correspondence between stress and strain. Hooke's law is used to describe the stress at a point resulting from a strain at this point. The strain itself results from a force displacing particles in the media. Hooke's law in terms of an incremental strain resulting in an incremental stress may be written as:

$$\begin{aligned} \dot{\sigma}_1 &= \frac{\dot{V}}{V} + 2\mu\dot{\epsilon}_1, \\ \dot{\sigma}_2 &= \frac{\dot{V}}{V} + 2\mu\dot{\epsilon}_2, \\ \dot{\sigma}_3 &= \frac{\dot{V}}{V} + 2\mu\dot{\epsilon}_3. \end{aligned} \tag{1}$$

Here λ and μ are the Lamé constants, and $\dot{\epsilon}_1$, $\dot{\epsilon}_2$, and $\dot{\epsilon}_3$ are the strain rates in the direction given by the subscripts; V = volume.

The dot means a time derivative along a particle path. It must be noted that the time derivative provides a desired ordered sequence for the incremental stress-strain relationship, but this does not mean that a rate-dependent stress-strain relationship has been introduced.[3] Hooke's law used in this way gives natural strain, which means that the strain of an element is referred to the current configuration instead of the original configuration.

The stress behavior of a material can be thought of as being composed of a stress associated with a uniform hydrostatic pressure (all three normal stresses equal) plus a stress associated with the resistance of the material to shear distortion. In describing yielding and plastic flow, we will want to

limit only the stress contributions that are due to shear distortions. Therefore, we will decompose each of the stresses σ_1, σ_2, and σ_3 into a hydrostatic component P and a deviator component s, where -P is the mean of three stresses: $-P = (1/3)\cdot(\sigma_1 + \sigma_2 + \sigma_3)$.

$$\begin{aligned} \sigma_1 &= -P + s_1 & & \dot{\sigma}_1 = -\dot{P} + \dot{s}_1 \\ \sigma_2 &= -P + s_2 & \text{also} \quad & \dot{\sigma}_2 = -\dot{P} + \dot{s}_2 \\ \sigma_3 &= -P + s_3 & & \dot{\sigma}_3 = -\dot{P} + \dot{s}_3. \end{aligned} \tag{2}$$

The usual notation is followed here such that stresses are >0 in tension and <0 in compression, which is just the opposite for pressure; hence the negative sign in front of the pressure. We will define the mean normal strain[1] as:

$$\theta = \frac{1}{3}(\epsilon_1 + \epsilon_2 + \epsilon_3) \qquad \text{also} \qquad \dot{\theta} = \frac{1}{3}(\dot{\epsilon}_1 + \dot{\epsilon}_2 + \dot{\epsilon}_3). \tag{3}$$

The normal components of the strain deviators are defined as:

$$\begin{aligned} \theta_1 &= \epsilon_1 - \theta & & \dot{\theta}_1 = \dot{\epsilon}_1 - \dot{\theta} \\ \theta_2 &= \epsilon_2 - \theta & \text{also} \quad & \dot{\theta}_2 = \dot{\epsilon}_2 - \dot{\theta} \\ \theta_3 &= \epsilon_3 - \theta & & \dot{\theta}_3 = \dot{\epsilon}_3 - \dot{\theta}. \end{aligned} \tag{4}$$

From the equation of continuity we have:

$$\dot{\epsilon}_1 + \dot{\epsilon}_2 + \dot{\epsilon}_3 = \frac{\dot{V}}{V}. \tag{5}$$

It follows that:

$$\dot{\theta}_1 + \dot{\theta}_2 + \dot{\theta}_3 = 0$$

and

$$\dot{\theta} = \frac{1}{3}\frac{\dot{V}}{V}.$$

Using the above definitions we may now write Hooke's law [Eq. (1)] as:

$$\begin{aligned} \dot{s}_1 &= 2\mu\left(\dot{\epsilon}_1 - \frac{1}{3}\frac{\dot{V}}{V}\right) \\ \dot{s}_2 &= 2\mu\left(\dot{\epsilon}_2 - \frac{1}{3}\frac{\dot{V}}{V}\right) \\ \dot{s}_3 &= 2\mu\left(\dot{\epsilon}_3 - \frac{1}{3}\frac{\dot{V}}{V}\right) \\ \dot{P} &= -K\frac{\dot{V}}{V} \qquad K = \left(\lambda + \frac{2}{3}\mu\right) = \text{bulk modulus}. \end{aligned} \tag{6}$$

Also from equations 5 and 6, it follows that:

$$\dot{s}_1 + \dot{s}_2 + \dot{s}_3 = 0 \tag{7}$$

and

$$s_1 + s_2 + s_3 = 0 \tag{8}$$

which says that the distortion components of the stresses do not contribute to the average pressure.

B. Plastic Flow Region

The yield condition of R. Von Mises is used to describe the elastic limit (see Ref. 4 for an English translation of the Von Mises paper). When the principal stresses are known, the yield condition can be written as:

$$(\sigma_1 - \sigma_2)^2 + (\sigma_2 - \sigma_3)^2 + (\sigma_3 - \sigma_1)^2 = 2(Y^0)^2 \tag{9}$$

where Y^0 is the yield strength in simple tension.

The left side of this expression is proportional to the elastic energy of distortion per unit volume or the energy required to change shape as opposed to the energy that causes a volume change (Ref. 5, p. 210). The expression states, therefore, that plastic flow begins when the elastic distortion energy reaches a limiting value $[(Y^0)^2/6\mu]$ and that this energy remains constant during the plastic flow. Thus, by the term "elastic-plastic" is meant the state whereby the distortion (change in shape) component of the strained material has been loaded, following Hooke's law, up to a state where the material can no longer store elastic energy. All subsequent distortion will produce plastic flow and plastic work will be done. The left side of Eq. (9) can also be interpreted in terms of shear strength. There are several ways of viewing Eq. (9), but the point here is that at the elastic limit the left side is equal to a constant. We have chosen to interpret the constant in terms of the yield strength in simple tension Y^0. If the tension is applied in the σ_1 direction and the lateral stresses σ_2 and σ_3 are zero, then Eq. (9) gives $\sigma_1 = Y^0$. The simple tension implies two-dimensional flow since in order for the lateral stresses to be zero there must be strains in the lateral directions. In fact the ratio $\dot{\epsilon}_2/\dot{\epsilon}_1$ for this case is Poisson's ratio, also, it is noted that Eq. (9) implies that the yield strength in tension is the same as the yield strength in compression (absence of Bauschinger effect).

In σ_1, σ_2, σ_3 space, Eq. (9) describes the surface of a straight circular cylinder. The axis of the cylinder is equally inclined to the σ_1, σ_2, σ_3 system of coordinates as shown in Fig. 1a. The radius of the cylinder is $\sqrt{2/3}\, Y^0$. We are going to use the principal stress deviators such that $s_1 + s_2 + s_3 = 0$ [see Eq. (8)]. This is the equation of a plane through the origin of the axes of the principal stresses. The intersection of this plane with the cylinder of Eq. (9) results in a circle (see Fig. 1a). If the stress deviators s_1, s_2, s_3 give a point inside the circle, the material is within the elastic limit.

When the material is loaded beyond the yield strength and subsequently unloaded, only the elastic distortion energy is recovered. The work done against the material while in the plastic state is not recovered. Another way of stating this is that the loading and unloading paths are not the same when the material has been loaded beyond the elastic limit (in Fig. 2a the loading path is OAB, the unloading path is BC). It has been demonstrated by D. C. Drucker[6] that: The work done on the material during a loading and unloading cycle must be positive or zero; zero only when purely elastic changes take place. Furthermore, the plastic strain increment must be normal to the yield surface that separates the elastic and the elastic-plastic states. We will describe plastic flow by maintaining the stress deviators (s_1, s_2, s_3) at the elastic limit. In Fig. 1b the stresses are shown at state n and after an incremental strain we will consider that the stresses have changed to state n + 1. However, state n + 1 is outside the yield circle and our assumption is that this state can not be reached. Instead, we will consider that the material flows plastically, but the stresses remain at the elastic limit on the yield circle. The plastic component of strain is perpendicular to the yield curve and it is the stress associated with this component of strain that we want to limit. Therefore, the new stress state, instead of being n + 1, is the point that is reached by a vector from n + 1 and perpendicular to the yield circle. The one-dimensional analogy is seen in Fig. 2b where the stress, $-s_1$, has a maximum value for all strains beyond the elastic limit point A. Thus, to summarize the yield assumption:

$$(s_1 - s_2)^2 + (s_2 - s_3)^2 + (s_3 - s_1)^2 \leq 2(Y^0)^2 \qquad (10)$$

$$s_1 + s_2 + s_3 = 0$$

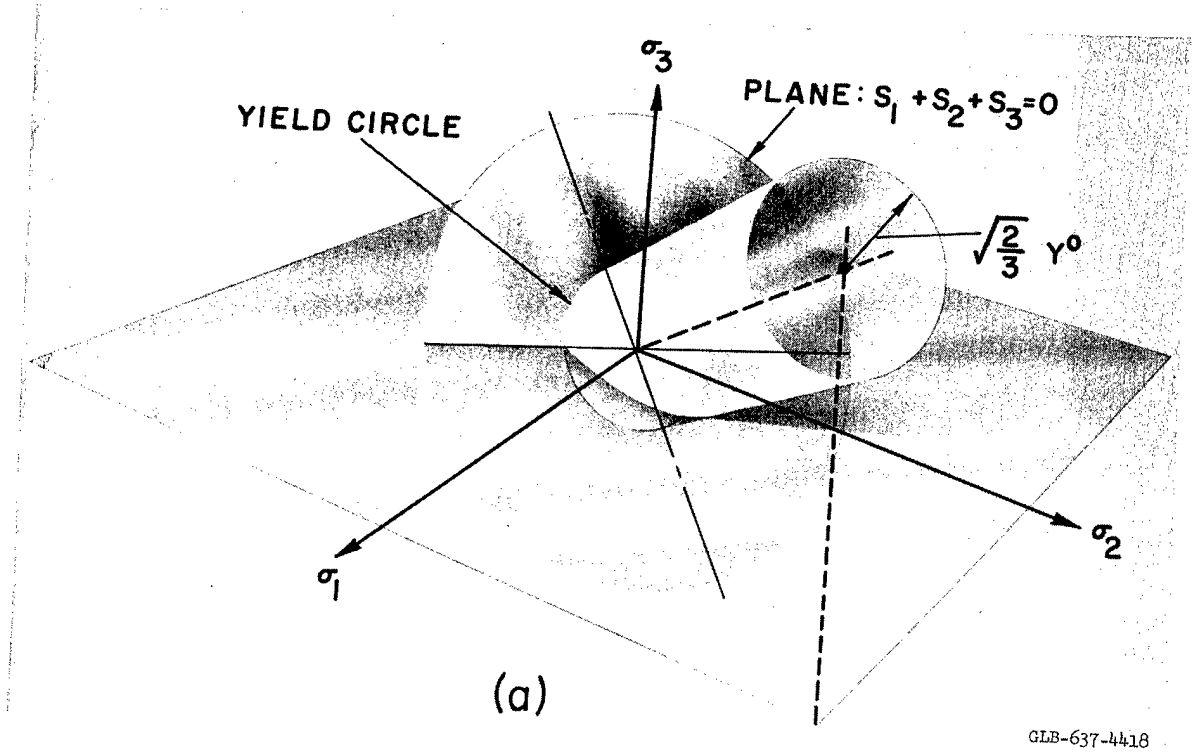

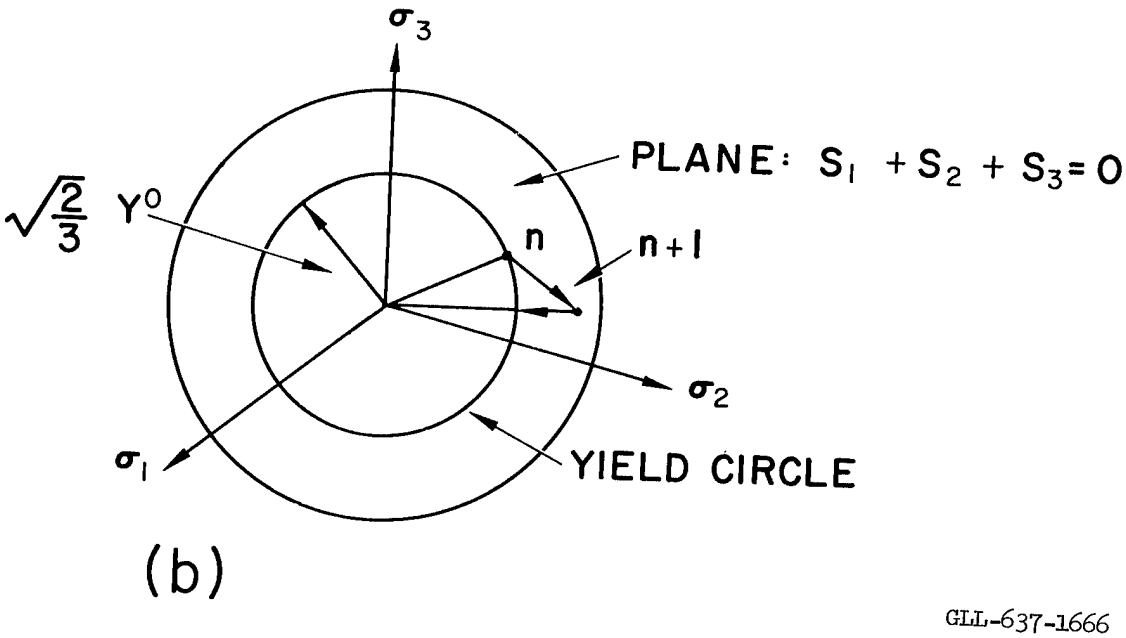

Fig. 1. Von Mises yield assumption.

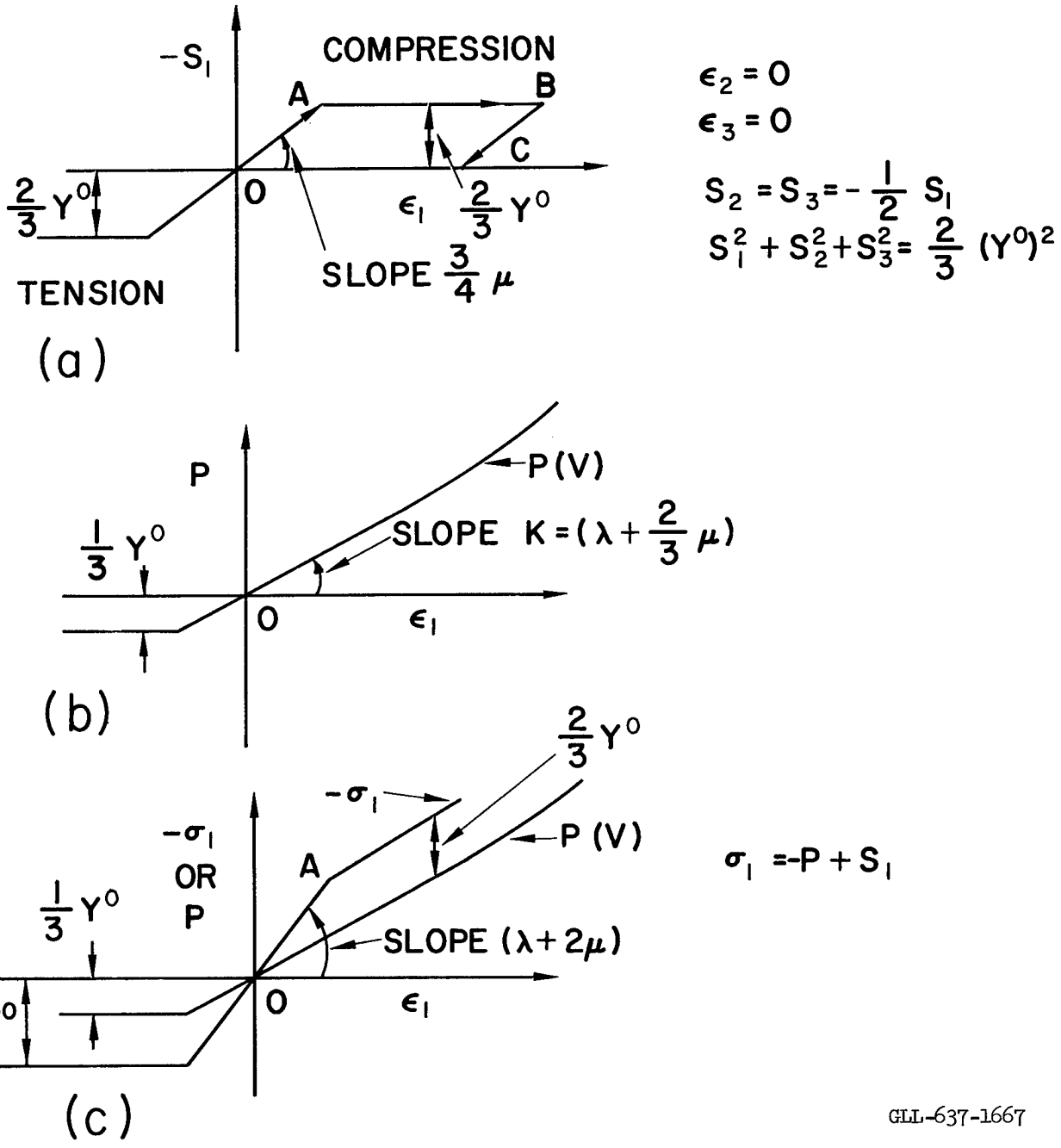

Fig. 2. One-dimensional strain for a perfectly plastic material.

which can be written as:

$$s_1^2 + s_2^2 + s_3^2 \leq 2/3\ (Y^0)^2 \tag{11}$$

If an incremental change in the stresses in an element results in a violation of the inequality, then each of the principal stress deviators (s_1, s_2, s_3) must be adjusted such that Eq. (11) is again satisfied. Hooke's law is used to calculate the stress deviators [Eq. (6)]. If a point falls outside the yield circle (Fig. 1b) it is brought back to the circle along the radius vector of the point and hence perpendicular to the yield circle. This is accomplished by multiplying each of the stress deviators (s_1, s_2, s_3) by $\sqrt{2/3}\ Y^0 \sqrt{s_1^2 + s_2^2 + s_3^2}$. By adjusting the stresses perpendicular to the yield circle, only the plastic components of the stresses are affected. The observed incompressibility of the plastic state is implicit in this procedure. Note that there is always a background pressure stress present, whether the material is in an elastic or an elastic-plastic state, but it is independent of the plastic flow. This is in agreement with the observed behavior of ductile metals. The above formulation corresponds to a perfectly plastic material, i. e. , material that flows plastically under a constant stress without work-hardening (see Fig. 2). For a work-hardening material the stress ($-s_1$) will increase monotonically with strain (ϵ_1) for strains beyond point A instead of remaining constant as for the perfectly plastic material shown. Work hardening can be introduced into the calculation by making the constant Y^0 in Eq. (9) a function of the strain energy, for example. Also, when enough work has been done to melt the material, the value of Y^0 can be set to zero. In this way an all-hydrodynamic description will follow since the stress deviators will automatically be set to zero by the above procedure and the only remaining stress will be the pressure P. Time-dependent yielding can be macroscopically represented by selecting a high yield constant Y^0 if the strain rates ($\dot{\epsilon}_1$, $\dot{\epsilon}_2$, $\dot{\epsilon}_3$) are above some prescribed value.

In the negative pressure region, the pressure is cut off at $P = -(1/3)Y^0$ consistent with a simple tension test.

The complete equation of state is given by:

$$\text{(i)}\begin{cases}\sigma_1 = -P + s_1\\ \sigma_2 = -P + s_2\\ \sigma_3 = -P + s_3\end{cases}\qquad \text{(ii)}\begin{cases}\dot{s}_1 = 2\mu\left[\dot{\epsilon}_1 - \frac{1}{3}\frac{\dot{V}}{V}\right]\\ \dot{s}_2 = 2\mu\left[\dot{\epsilon}_2 - \frac{1}{3}\frac{\dot{V}}{V}\right]\\ \dot{s}_3 = 2\mu\left[\dot{\epsilon}_3 - \frac{1}{3}\frac{\dot{V}}{V}\right]\end{cases}\qquad \begin{aligned}&\text{(iii)}\quad s_1^2 + s_2^2 + s_3^2 \le \tfrac{2}{3}(Y^0)^2\\ &\text{(iv)}\quad s_1 + s_2 + s_3 = 0\\ &\text{(v)}\quad P = P(V)\\ &\text{(vi)}\quad \text{Minimum } P = -\tfrac{1}{3}Y^0\end{aligned} \tag{12}$$

C. Experimental Equation of State

Consider a one-dimensional shock traversing a material such that there is a strain in the X direction and zero strains in the Y and Z directions. This is the geometry whereby Hugoniot equation-of-state data are obtained. A shock exists that takes the material through an elastic to an elastic-plastic state.[7]

For one-dimensional flow, the X, Y, Z coordinates are the principal directions, so by Eqs. (6) the three stress deviators s_x, s_y, s_z are:

$$\begin{aligned}\dot{s}_x &= 2\mu\left(\dot{\epsilon}_x - \frac{1}{3}\frac{\dot{V}}{V}\right)\\ \dot{s}_y &= 2\mu\left(0 - \frac{1}{3}\frac{\dot{V}}{V}\right)\\ \dot{s}_z &= 2\mu\left(0 - \frac{1}{3}\frac{\dot{V}}{V}\right).\end{aligned} \tag{13}$$

The total stress in the X direction is:

$$\sigma_x = -P + s_x. \tag{14}$$

We will assume it is σ_x that is obtained by Hugoniot measurements.

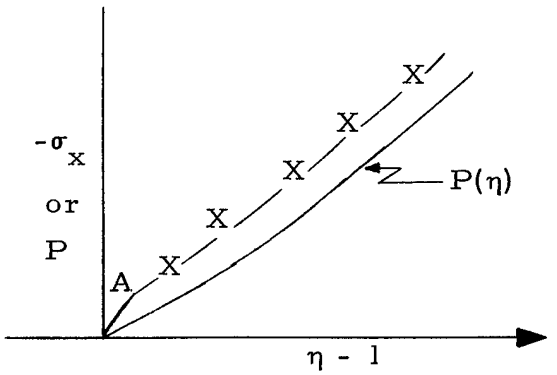

X-X - Hugoniot

A - Hugoniot elastic limit

$\eta = \rho/\rho^0 = 1/V$

ρ^0 = reference density

ρ = actual density

Fig. 3

For 1-D flow the equation of continuity gives $\dot{\epsilon}_x = \dot{V}/V$. The complete equation of state for one-dimensional geometry is described by:

$$\text{(i)} \quad \sigma_x = -P + s_x \qquad \text{(iv)} \quad s_x + 2s_y = 0$$

$$\text{(ii)} \begin{cases} \dot{s}_x = 2\mu\left[\dfrac{\dot{V}}{V} - \dfrac{1}{3}\dfrac{\dot{V}}{V}\right] \\ \dot{s}_y = 2\mu\left[-\dfrac{1}{3}\dfrac{\dot{V}}{V}\right] \end{cases} \qquad \text{(v)} \quad P = P(V)$$

$$\text{(iii)} \quad \left(s_x^2 + 2s_y^2\right) \leq \frac{2}{3}\left(Y^0\right)^2 \qquad \text{(vi)} \quad \text{Minimum } P = -\frac{1}{3}Y^0. \tag{15}$$

Up to the elastic limit, point A, we have:

$$P = -K\frac{\dot{V}}{V} \qquad \text{and} \qquad \dot{s}_x = 2\mu\left[\dot{V}/V - (1/3)\dot{V}/V\right]$$

or

$$P = -K \ln V \qquad \text{and} \qquad s_x = (4/3)\mu \ln V = -2s_y \tag{16}$$

$$\sigma_x = K \ln V + \frac{4}{3}\mu \ln V$$

$$= \left(K + \frac{4}{3}\mu\right)\ln V.$$

At point A:

$$\left(s_x^2 + 2s_y^2\right)_A = \frac{2}{3}\left(Y^0\right)^2$$

or

$$(24/9)(\mu \ln V_A)^2 = \frac{2}{3}\left(Y^0\right)^2$$

$$Y^0 = 2\mu\left|\ln V_A\right| = \frac{2\mu(\sigma_x)_A}{\lambda + 2\mu}. \tag{17}$$

This gives the maximum yield strength Y^0 if the Lamé constants and the Hugoniot elastic limit are known.

For points beyond A we have: $\left(s_x^2 + 2s_y^2\right) = \frac{2}{3}\left(Y^0\right)^2$ which reduces to:

$$s_x = \pm\frac{2}{3}Y^0 \qquad \text{[from (iv) Eq. (15)]}, \tag{18}$$

[if the material yields in tension, $s_x > 0$, in compression, $s_x < 0$ (Y^0 is always > 0)]

so the total stress resulting from a shock from $\sigma_x = 0$ to a value above point A is:

$$- \sigma_x = P(V) + \frac{2}{3}(Y^0) \tag{19}$$

P(V) can be expressed conveniently as:

$$P(\eta) = a(\eta - 1) + b(\eta - 1)^2 + c(\eta - 1)^3. \tag{20}$$

Here a, b, and c are constants such that $P(\eta) + (2/3)Y^0$ reproduces the Hugoniot for shocks above the elastic limit and $P(\eta) = -K \ln V$ for pressures below the elastic limit.

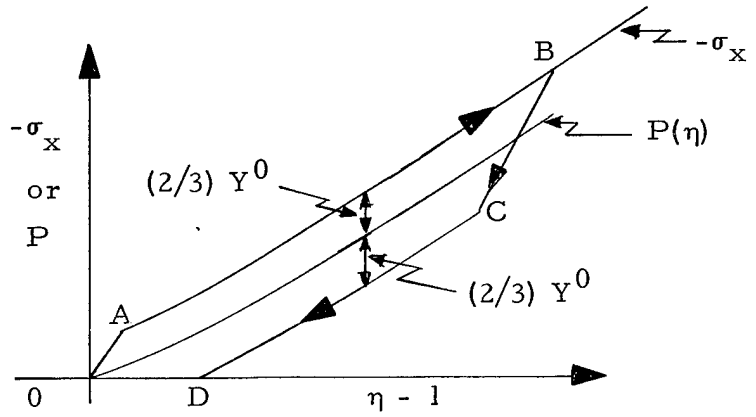

Fig. 4

The result of using an equation of state as given by Eqs. (15) is a loading path O, A, B (Fig. 4) and an unloading path B, C, D. Experiments on metals in the low-pressure range (0 → 50 kb) have demonstrated the difference between the hydrostatic $P(\eta)$ and the Hugoniot (σ_x) curves. At high pressures (hundreds of kilobars) for some metals the sound speed behind the shock has been measured to be of the order of 20% faster than that predicted by hydrodynamic theory. This gives reason to extend the low-pressure model up to high pressures. Upon unloading from a high pressure, the material unloads first elastically along BC; the slope of this path is characteristic of the elastic unloading velocity. Consequently, the rarefaction travels faster than would be the case if the material unloaded entirely along the $P(\eta)$ path.

Experiments that have measured high sound speed behind shocks in metals have been performed in Russia,[8] Stanford Research Institute, and at this Laboratory.

Using Hugoniot data of J. M. Walsh[9] and the elastic data of C. D. Lundergan,[10] the constants for Eqs. (12) for aluminum are:

$$Y^0 = 0.002976 \text{ mb} \qquad \text{(from Eq. (17) with } (\sigma_x)_A = 0.0063 \text{ mb and } V_A = 0.994\text{)}$$

$$\mu = 0.248 \text{ mb}$$

$$P = 0.73\,(\eta - 1) + 1.72\,(\eta - 1)^2 + 0.40\,(\eta - 1)^3$$

$$\rho^0 = 2.7.$$

Figures 5 and 6 show the results of finite difference calculations of a flying aluminum plate striking a target plate. The calculation shows that even though the yield strength Y^0 is small compared to the total stress σ_x, the effect on the wave is very pronounced.

In principle, calculations of this type in conjunction with experiments could be used in determining the properties of materials at high pressure based on the model described by Eqs. (12). Front-surface velocity measurements for various thicknesses of target plates could determine when the elastic wave overtakes the shock front (see Fig. 6) and this would establish the slope of BC in Fig. 4. The magnitude of the step behind the shock in Fig. 6 would correspond to point C of Fig. 4.

If the material behaves entirely hydrodynamically, then the step behind the shock front will not be present. In Fig. 5 it is seen that the rarefaction due to the hydrodynamic unloading is proceeding much slower than the elastic unloading. The hydrodynamic rarefaction however, can be seen to be overtaking the shock front from the increase in the slant of the rear of the wave as time increases.

It should be noted that to account for high sound speeds behind a shock it is only necessary to postulate that the material unloads first elastically and then plastically. The result would still follow even though at high pressures the $-\sigma_x$ curve merged with the $P(\eta)$ curve. We have maintained the values of Y^0 and μ constant in these calculations since the details of the elastic unloading from high pressures are not known.

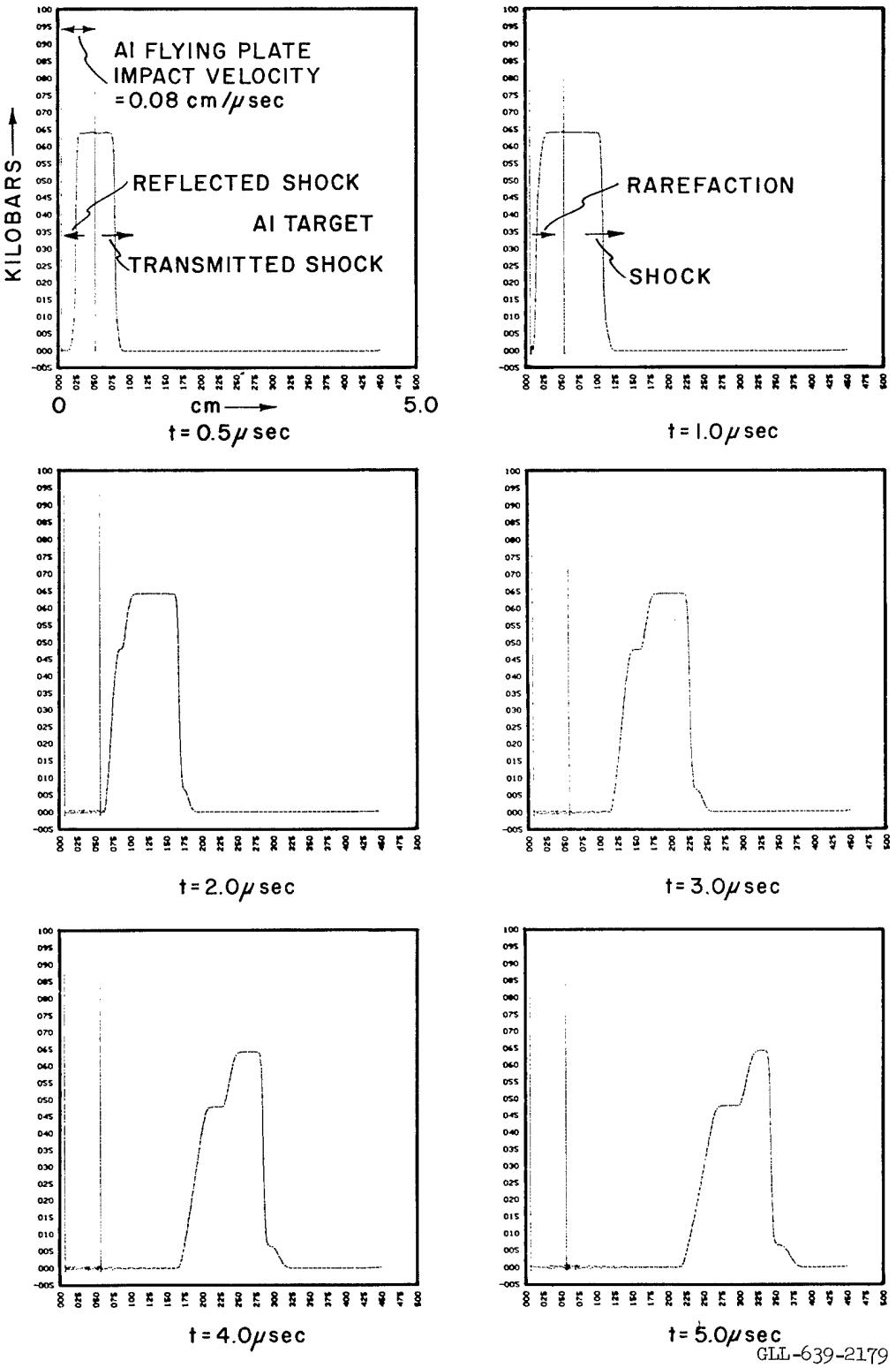

Fig. 5. Stresses from a flying plate striking a target plate.

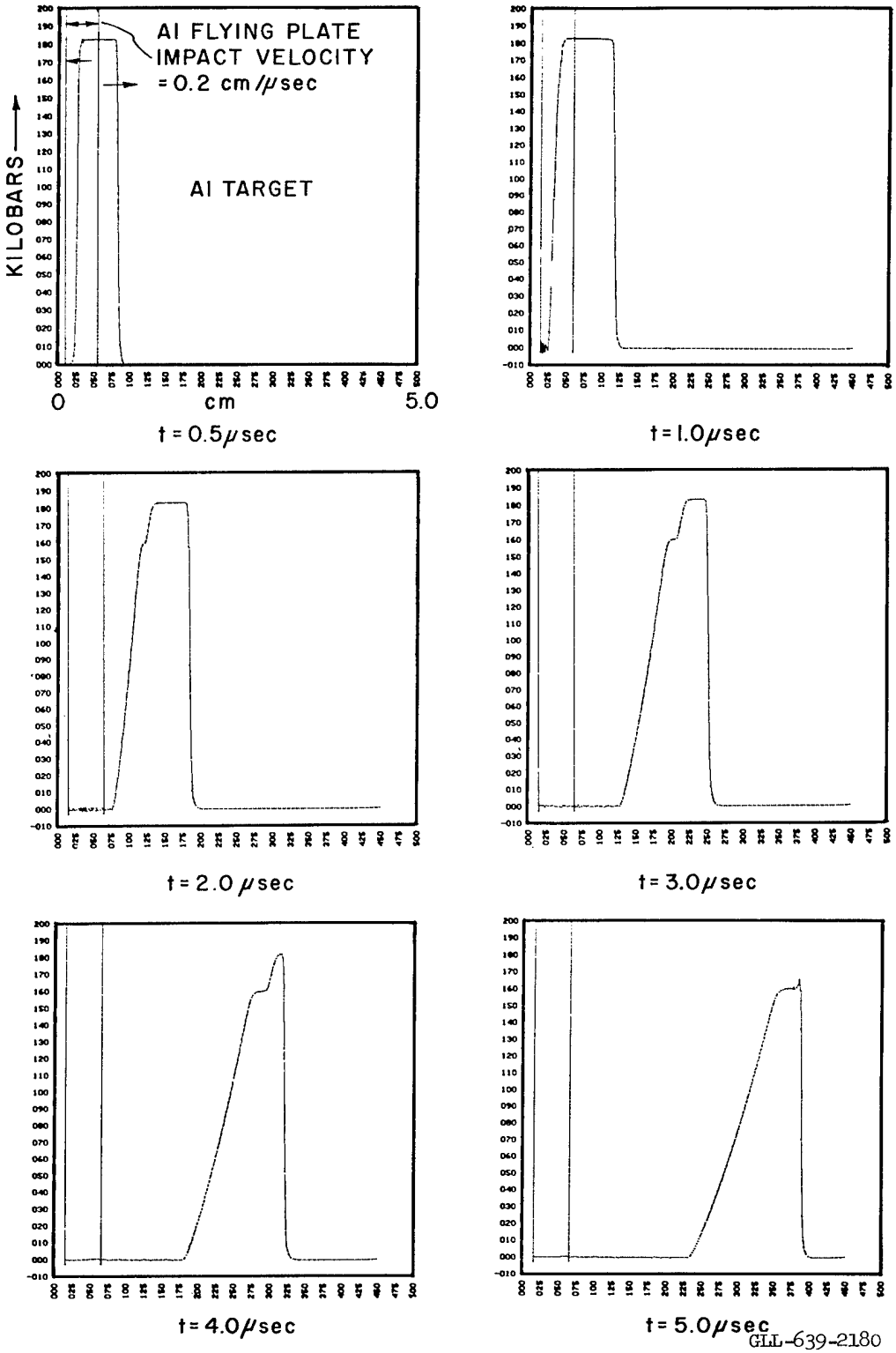

Fig. 6. Stresses from a flying plate striking a target plate.

PART II. ONE-DIMENSIONAL ELASTIC-PLASTIC FLOW

For time-dependent flow in one space variable (r), the principal equations for plane (d = 1), cylindrical (d = 2), and spherical (d = 3) geometries are:

equation of motion

$$\frac{\rho^0 \dot{U}}{V} = \frac{\partial \Sigma_r}{\partial r} + (d - 1)\frac{\Sigma_r - \Sigma_\theta}{r} \tag{21}$$

$$\Sigma_r = -(P + q) + s_1$$

$$\Sigma_\theta = -(P + q) + s_2$$

equation of continuity

$$\frac{\dot{V}}{V} = \frac{1}{r^{d-1}}\frac{\partial (r^{d-1} U)}{\partial r} \tag{22}$$

energy equation

$$\dot{E} - V\left[s_1 \dot{\epsilon}_1 + (d - 1)\, s_2 \dot{\epsilon}_2\right] + (P + q)\,\dot{V} = 0 \tag{23}$$

artificial viscosity (linear q)

$$q = C^0 \frac{\rho^0}{V}\left(\frac{\partial U}{\partial r}\right)\Delta r \qquad C^0 = \text{constant} \tag{24}$$

equation of state

anisotropic stresses

$$\begin{cases} s_1 = 2\mu\left(\dot{\epsilon}_1 - \frac{1}{3}\frac{\dot{V}}{V}\right) \\ s_2 = 2\mu\left(\dot{\epsilon}_2 - \frac{1}{3}\frac{\dot{V}}{V}\right) \\ s_3 = 2\mu\left(\dot{\epsilon}_3 - \frac{1}{3}\frac{\dot{V}}{V}\right) \end{cases} \tag{25}$$

NOTE: Three stresses are identified here, even though they are not all required, so as to maintain an analogy with the two-dimensional calculations in Part III.

velocity strains

$$\begin{cases} \dot{\epsilon}_1 = \frac{\partial U}{\partial r} \\ \dot{\epsilon}_2 = \frac{U}{r} \\ \dot{\epsilon}_3 = \dot{\epsilon}_2 \text{ for } d = 3 \\ \dot{\epsilon}_3 = 0 \text{ for } d = 2 \\ \dot{\epsilon}_3 = \dot{\epsilon}_2 = 0 \text{ for } d = 1 \end{cases}$$

hydrostatic pressure

$$P = a(\eta - 1) + b(\eta - 1)^2 + c(\eta - 1)^3 + d\eta E$$

$$\eta = \frac{1}{V} = \frac{\rho}{\rho^0}$$

Von Mises yield condition

$$\left(s_1^2 + s_2^2 + s_3^2\right)^{n+1} - (2/3)(Y^0)^2 \leq 0 \qquad Y^0 = \text{material strength}$$

Notation:

r	space coordinate
U	velocity in r direction
Σ_r, Σ_θ	total stresses
s_1, s_2, s_3	stress deviators
ϵ_1, ϵ_2, ϵ_3	strains
P	hydrostatic pressure
V	relative volume
ρ^0	reference density
ρ	actual density
E	internal energy per original volume

The dot over a parameter signifies a time derivative along the particle path.

Application

The finite difference equations for the above set of partial differential equations are given in Appendix A.

Figure 5 shows a calculation in plane geometry (d = 1) of a flying plate coming from the left with a velocity U = 0.08 cm/μsec and striking a target at rest. The materials are aluminum, with the constants given in Part I. At this impact velocity the elastic signal travels faster than the shock speed and the shock breaks into two components. In Fig. 6 the same problem has been calculated with a higher impact velocity (0.2 cm/μsec). In this case the shock speed is greater than the elastic signal speed and the shock front is the same as though the material were following an all hydrodynamic descriptions. However, it can be seen that the elastic relief wave that originated from the rear of the flying plate is overtaking the shock front.

Figure 7 shows the stress waves resulting from a 1-cm-radius spherical charge of high explosive (comp. B) detonated at the center.[11] The region from 1 cm to 5 cm is treated as an elastic material with $P = K(\eta - 1)$, $K = 1.39$ mb, $\rho^0 = 8.9$, $\mu = 0.46$ mb, and $Y^0 = \infty$. The stress waves are traveling at a velocity $C = [(K + \frac{4}{3}\mu)/\rho^0]^{1/2}$ cm/μsec. A second shock can be seen that has originated from the high-explosive cavity.[12]

The second shock is a hydrodynamic effect and is not a result of the elastic property of the material. The radial stress is seen to be followed by a tension tail of about -10 kb. The tension is due entirely to the elastic property of the material. If the material were described by hydrodynamics alone, there would not be a tension portion behind the outward-travelling pressure stress wave.

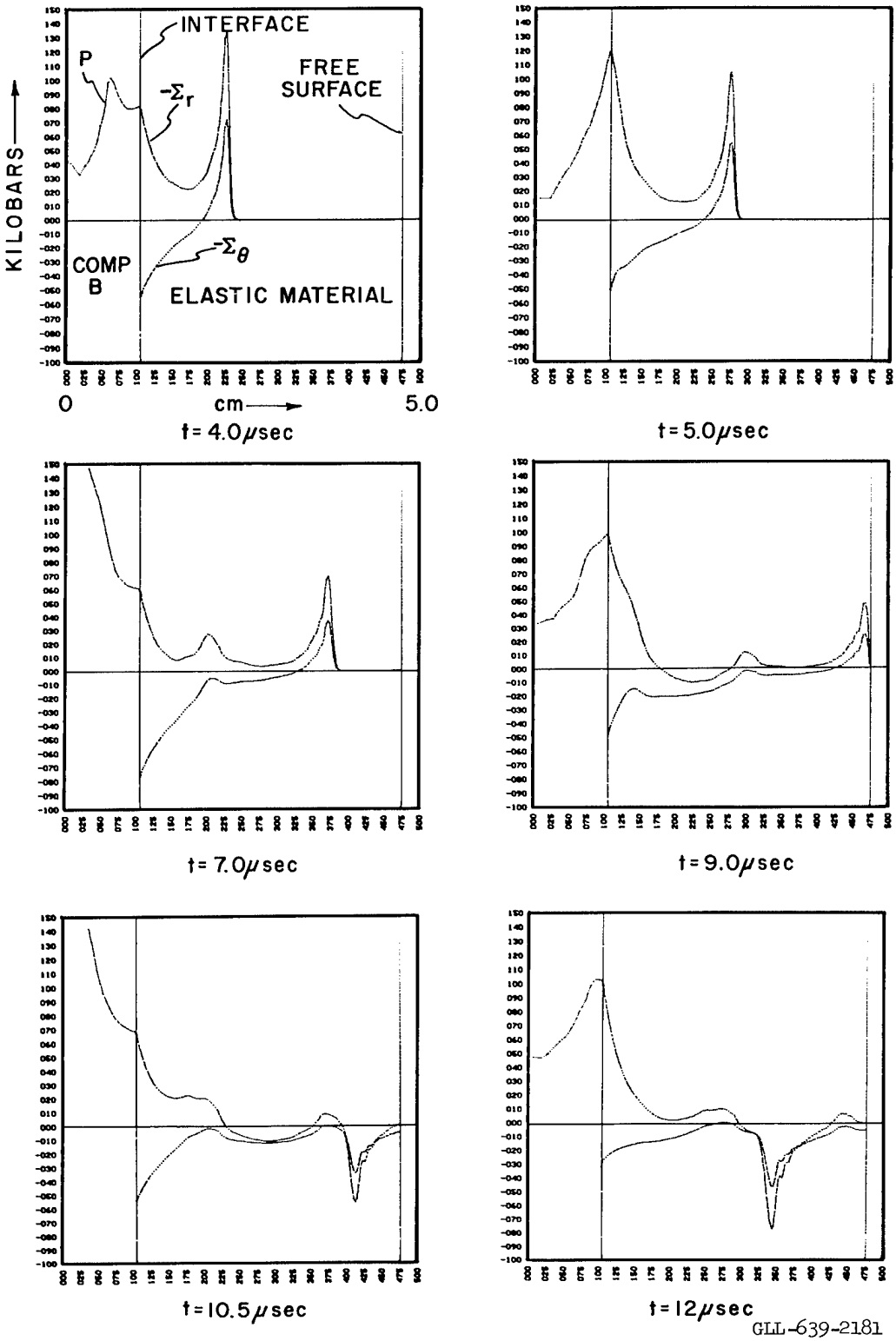

Fig. 7. Spherically diverging elastic waves.

PART III. TWO-DIMENSIONAL ELASTIC-PLASTIC FLOW

The equations of motion listed below are those used by the HEMP code, a program that solves the equations by finite difference techniques on the IBM 7030 electronic computer. The derivation of the equations can be found in Ref. 13. The problem is formulated in Lagrange coordinates with sliding interfaces allowed between an elastic and a hydrodynamic region or between two hydrodynamic regions, but not between two elastic regions. However, an elastic region may slide along a fixed boundary. The equation of state is used in the same manner as described in the preceeding sections. There is, however, the additional complication that the stress-strain relationship must be independent of a rigid motion and hence the incremental stress-strain relationship must be corrected for a rotation in the x-y coordinate system (Ref. 14). When a zone is displaced from an initial state of stress, there may be a rotation through an angle ω as well as a distortion. The rotation will not contribute to an increase in stress, but the state of stress $\left(s^n_{xx}, s^n_{yy}, T^n_{xy}\right)$ originally in the zone has been rotated through the angle ω. Since the equations of motion are referred to the fixed x-y coordinate system, the rotated stresses must be recalculated in terms of the coordinate system. The transformation equations (Ref. 5, p. 110) result in a correction δ that is added to the stresses. The stresses can then be incremented by the strain that occurred between time t^n and time t^{n+1} to give the stresses at time t^{n+1}. The rotation angle is given by:

$$\sin \omega = \frac{1}{2} \left(\frac{\partial \dot{y}}{\partial x} - \frac{\partial \dot{x}}{\partial y} \right) \Delta t^{n+1/2} .$$

It is not practical to increment the stresses in the principal stress coordinate system because the principal stress directions are not unique and also there can be large changes in directions between two consecutive time steps. Therefore, the operation of transforming to the principal stress coordinate system and then back to the x-y coordinate system every cycle would become complicated and inaccurate. Even though the program to be described does make the transformation to the principal stress system to test for yielding, the directions of the principal stresses are not required in the calculations and the complications involving these directions is avoided. (The Von Mises yield condition can be used without reference to the principal stresses (see Appendix B 7-b), however, the geometrical interpretation of the yielding is easier if the principal stress deviators are used instead of the stress deviators.)

A. Basic Equations in the HEMP Code

Equations of motion in x-y coordinates with cylindrical symmetry about the x-axis (it is desirable to have the problem formulated also in plane x-y coordinates; for this case the terms marked $\Big|^*$ are set = 0):

$$\left.\frac{\partial \Sigma_{xx}}{\partial x} + \frac{\partial T_{xy}}{\partial y} + \frac{T_{xy}}{y}\right|^* = \rho \ddot{x} \ ,$$

$$\left.\frac{\partial T_{xy}}{\partial x} + \frac{\partial \Sigma_{yy}}{\partial y} + \frac{\Sigma_{yy} - \Sigma_{\theta\theta}}{y}\right|^* = \rho \ddot{y} \ ,$$

$$\Sigma_{xx} = s_{xx} - (P + q), \tag{26}$$

$$\Sigma_{yy} = s_{yy} - (P + q),$$

$$\Sigma_{\theta\theta} = s_{\theta\theta} - (P + q).$$

Equation of continuity:

$$\frac{\dot{V}}{V} = \left.\frac{\partial \dot{x}}{\partial x} + \frac{\partial \dot{y}}{\partial y} + \frac{\dot{y}}{y}\right|^* . \tag{27}$$

Energy equation:

$$\dot{E} = - (P + q)\, \dot{V} + V\left(s_{xx}\dot{\epsilon}_{xx} + s_{yy}\dot{\epsilon}_{yy} + s_{\theta\theta}\dot{\epsilon}_{\theta\theta} + T_{xy}\dot{\epsilon}_{xy}\right) . \tag{28}$$

Artificial viscosity: (quadratic "q")

$$q = C_0^2\, \rho^0 (\dot{V}/V)^2\, A/V \tag{29}$$

where

C^0 = constant

A = zone area

ρ^0 = reference density.

Equation of state:

$$\text{stress components} \begin{cases} \dot{s}_{xx} = 2\mu\left(\dot{\epsilon}_{xx} - \frac{1}{3}\frac{\dot{V}}{V}\right) + \delta_{xx}, \\ \dot{s}_{yy} = 2\mu\left(\dot{\epsilon}_{yy} - \frac{1}{3}\frac{\dot{V}}{V}\right) + \delta_{yy}, \\ \dot{s}_{\theta\theta} = 2\mu\left(\dot{\epsilon}_{\theta\theta} - \frac{1}{3}\frac{\dot{V}}{V}\right), \\ T_{xy} = \mu(\dot{\epsilon}_{xy}) + \delta_{xy}, \end{cases} \tag{30}$$

where

μ = shear modulus

δ = correction for rotation (see text).

$$\text{velocity strains} \quad \begin{cases} \dot{\epsilon}_{xx} = \dfrac{\partial \dot{x}}{\partial x} \quad \dot{\epsilon}_{\theta\theta} = \dfrac{\dot{y}}{y} \Big|^{*} \\ \dot{\epsilon}_{yy} = \dfrac{\partial \dot{y}}{\partial y} \quad \dot{\epsilon}_{xy} = \dfrac{\partial \dot{y}}{\partial x} + \dfrac{\partial \dot{x}}{\partial y} . \end{cases} \tag{31}$$

Hydrostatic pressure

$$P = a(\eta - 1) + b(\eta - 1)^2 + c(\eta - 1)^3 + d\eta E, \qquad \eta = 1/V = \rho/\rho^0. \tag{32}$$

Von Mises yield condition

$$\left(s_1^2 + s_2^2 + s_3^2\right) - (2/3)(Y^0)^2 \leq 0 \tag{33}$$

where

Y^0 = material strength

(s_1, s_2, s_3) are the principal stress deviators.

Notation:

x, y	space coordinates
$\dot{x}$	velocity in x direction
$\dot{y}$	velocity in y direction
$\Sigma_{xx}, \Sigma_{yy}, \Sigma_{\theta\theta}$	total stresses
T_{xy}	shear stress
$s_{xx}, s_{yy}, s_{\theta\theta}$	stress deviators
$\epsilon_{xx}, \epsilon_{yy}, \epsilon_{\theta\theta}, \epsilon_{xy}$	strains
P	hydrostatic pressure
V	relative volume
E	internal energy per original volume
ρ	density

The dot over a parameter signifies a time derivative along the particle path.

B. Finite Difference Scheme

The following integral definitions of the partial derivatives are used (see p. 327, Ref. 15):

$$\frac{\partial F}{\partial x} = \frac{\int_C F(\hat{n} \cdot \hat{i})\, dS}{\lim_{A \to 0} A} \tag{34}$$

$$\frac{\partial F}{\partial y} = \frac{\int_C F(\hat{n} \cdot \hat{j})\, dS}{\lim_{A \to 0} A} \tag{35}$$

where

C is the boundary of area A

S = arc length

$\hat{n}$ = normal vector

$\hat{t}$ = tangent vector.

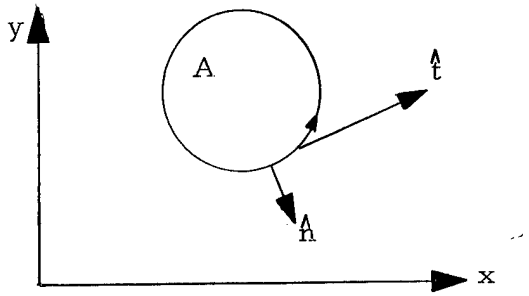

$$\hat{n} = \frac{\partial x}{\partial n}\hat{i} + \frac{\partial y}{\partial n}\hat{j} = \frac{\partial y}{\partial S}\hat{i} - \frac{\partial x}{\partial S}\hat{j}\,. \tag{36}$$

Applying the above to the quadrilateral 1, 2, 3, 4, we have for a parameter F defined at the points 1, 2, 3, and 4:

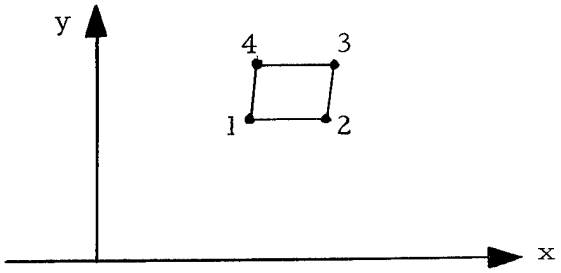

A = area of quadrilaterial

$$\int F(\hat{n} \cdot \hat{i})\, dS = + \int F \frac{\partial y}{\partial S}\, dS \tag{37}$$

$$= - \left[F_{23}(y_2 - y_3) + F_{34}(y_3 - y_4) + F_{41}(y_4 - y_1) + F_{12}(y_1 - y_2)\right] \tag{38}$$

where $F_{23} = (F_2 + F_3)/2$, etc.

$$\text{So } \frac{\partial F}{\partial x} = - \frac{1}{A}\left[F_{23}(y_2 - y_3) + F_{34}(y_3 - y_4) + F_{41}(y_4 - y_1) + F_{12}(y_1 - y_2)\right] \tag{39}$$

$$= + \frac{1}{2A}\left[(F_2 - F_4)(y_3 - y_1) - (y_2 - y_4)(F_3 - F_1)\right]\,.$$

Similarly

$$\frac{\partial F}{\partial y} = -\frac{1}{2A}\left[(F_2 - F_4)(x_3 - x_1) - (x_2 - x_4)(F_3 - F_1)\right]. \tag{40}$$

The quantities $\partial F/\partial x$ and $\partial F/\partial y$ are considered to be defined at the center of the quadrilateral.

Using the above difference equations we can now write an expression for $\partial\dot{x}/\partial x$ and $\partial\dot{y}/\partial y$ at a given time and position. The difference scheme to be used defines the velocities ($\dot{x}$ and $\dot{y}$) at 1/2 time increments and the space quantities (x and y) at integral time increments.

If we use the definitions:

$$x^{n+1/2} = 1/2\,(x^{n+1} + x^n), \text{ etc.}$$

and

$$A^{n+1/2} = 1/2\,(A^{n+1} + A^n)$$

where A^n and A^{n+1} = area of the quadrilateral at time t^n and time t^{n+1}, respectively, then the difference equations will give:

$$\frac{\partial\dot{x}}{\partial x} + \frac{\partial\dot{y}}{\partial y} \underline{\underline{\text{ exactly }}} \frac{\dot{A}}{A} \quad \text{(continuity equation in plane x-y geometry where } \dot{A}/A = \dot{V}/V\text{).} \tag{41}$$

It is obviously very desirable that a difference scheme have this property since it leads to zero truncation error in the numerical integration of each of the terms in Eq. (41).

We will now consider the continuity equation in x, y coordinates with cylindrical symmetry about the x axis.

$$\left[\frac{\partial\dot{x}}{\partial x} + \frac{\partial\dot{y}}{\partial y}\right] + \frac{\dot{y}}{y} = \frac{\dot{V}}{V}. \tag{42}$$

Here V is the volume swept out when the area A is rotated about the x axis.

$$V = \bar{y}_a A_a + \bar{y}_b A_b$$

A_a = area of Δa $\quad A = A_a + A_b$

A_b = area of Δb

$$\bar{y}_a = 1/3\,(y_2 + y_3 + y_4)$$

$$\bar{y}_b = 1/3\,(y_2 + y_4 + y_1) \tag{43}$$

$$\dot{y}_a = 1/3\,(\dot{y}_2 + \dot{y}_3 + \dot{y}_4)$$

$$\dot{y}_b = 1/3\,(\dot{y}_2 + \dot{y}_4 + \dot{y}_1)$$

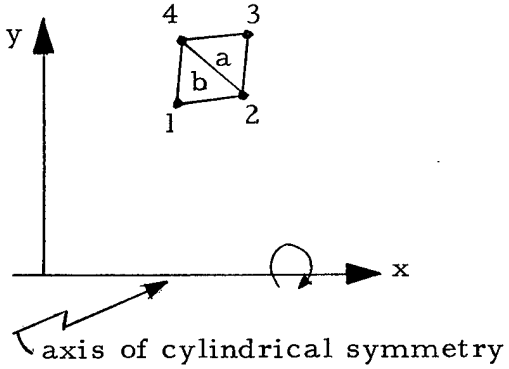

A very good approximation for the third term, $\dot{y}/y$, of Eq. (42) is given by:

$$\frac{\dot{y}}{y} = \frac{A_a^{n+1/2}\dot{y}_a + A_b^{n+1/2}\dot{y}_b}{A_a^{n+1/2}\bar{y}_a^{n+1/2} + A_b^{n+1/2}\bar{y}_b^{n+1/2}} \quad . \tag{44}$$

It is important to recognize that the difference equations for the terms in brackets in Eq. (42) are the same as for the left side of Eq. (41) i. e., they are independent of the coordinate system. Since there is essentially zero truncation error with the integration of these terms, it is possible to calculate $\dot{V}/V$ from the coordinates and express $\dot{y}/y$ as:

$$\frac{\dot{y}}{y} = \frac{\dot{V}}{V} - \left[\frac{\partial \dot{x}}{\partial x} + \frac{\partial \dot{y}}{\partial y}\right] \quad . \tag{45}$$

For the acceleration routines, the given parameter F in Eqs. (34) and (35) is defined at the center of a quadrilateral. The area enclosed in the integration is the area I, II, III, IV in the figure below.

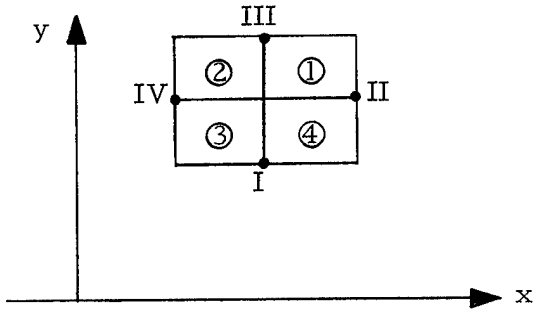

The corresponding difference equations for the $\hat{i}$ and $\hat{j}$ components of acceleration become:

$$\int F(\hat{n} \cdot \hat{i})\, dS = -\left[F_{①}(y_{II} - y_{III}) + F_{②}(y_{III} - y_{IV}) + F_{③}(y_{IV} - y_{I}) + F_{④}(y_{I} - y_{II})\right] , \tag{46}$$

$$\int F(\hat{n} \cdot \hat{j})\, dS = +\left[F_{①}(x_{II} - x_{III}) + F_{②}(x_{III} - x_{IV}) + F_{③}(x_{IV} - x_{I}) + F_{④}(x_{I} - x_{II})\right] . \tag{47}$$

The area I, II, III, IV is considered to be the mean of the quadrilateral areas $A_{①}$, $A_{②}$, $A_{③}$, and $A_{④}$. As can be seen in Appendix B, the quadrilaterals are weighted by the four corresponding densities.

C. Applications

The complete set of difference equations, including sliding interfaces and boundary conditions, is given in Appendix B. In the following figures, applications of these equations to specific problems are shown. The plots were made directly from the high-speed computer by a cathode ray tube and then photographed. Zones are shaded with an intensity weighted by the rate of zone compression. Hence, the shocks or detonation fronts are traced on the grid.

Figure 8 shows the time sequence of events due to a charge of explosive detonated at constant volume against a plate of copper. The horizontal line through the middle of the grid is an axis of cylindrical symmetry. The equation of state for the copper was derived in the same manner as previously discussed for aluminum. The yield strength used was Y^0 = 10 kb and shear modulus μ = 460 kb.

Figure 9 shows the directions of the maximum principal stresses for the above problem. The maximum principal stress with the sign convention being used is the tension component of the stresses. Therefore, the line segments point in a direction normal to the direction of an incident shock. By examining the plots, the progress of rarefactions from the free surfaces can be followed since the lines point in the direction of tensions.

Figure 10 shows the same problem, but the copper is described by a hydrodynamic equation of state with no strength of materials. It can be seen that the crater is much deeper than in the preceding problem. The crater lip is seen to increase with time. With a hydrodynamic description there are no restoring forces if the material deforms at constant volume. The elastic-plastic description gives rise to restoring forces that resist a change in shape even though the volume remains constant, and hence no lip is formed for the problem shown in Fig. 8. A lip will form, however, for calculations made with yield strengths of 1 to 2 kilobars.

Figures 11 and 12 show the time sequence of stresses in a copper plate resulting from the interactions of detonation fronts in a high explosive (PBX 9404). The calculation was made in plane geometry and the detonation centers are lines perpendicular to the page on the right- and left-hand lower corners. The left- and right-hand boundaries are planes of symmetry. The copper has a yield strength Y^0 = 10 kb in this calculation.

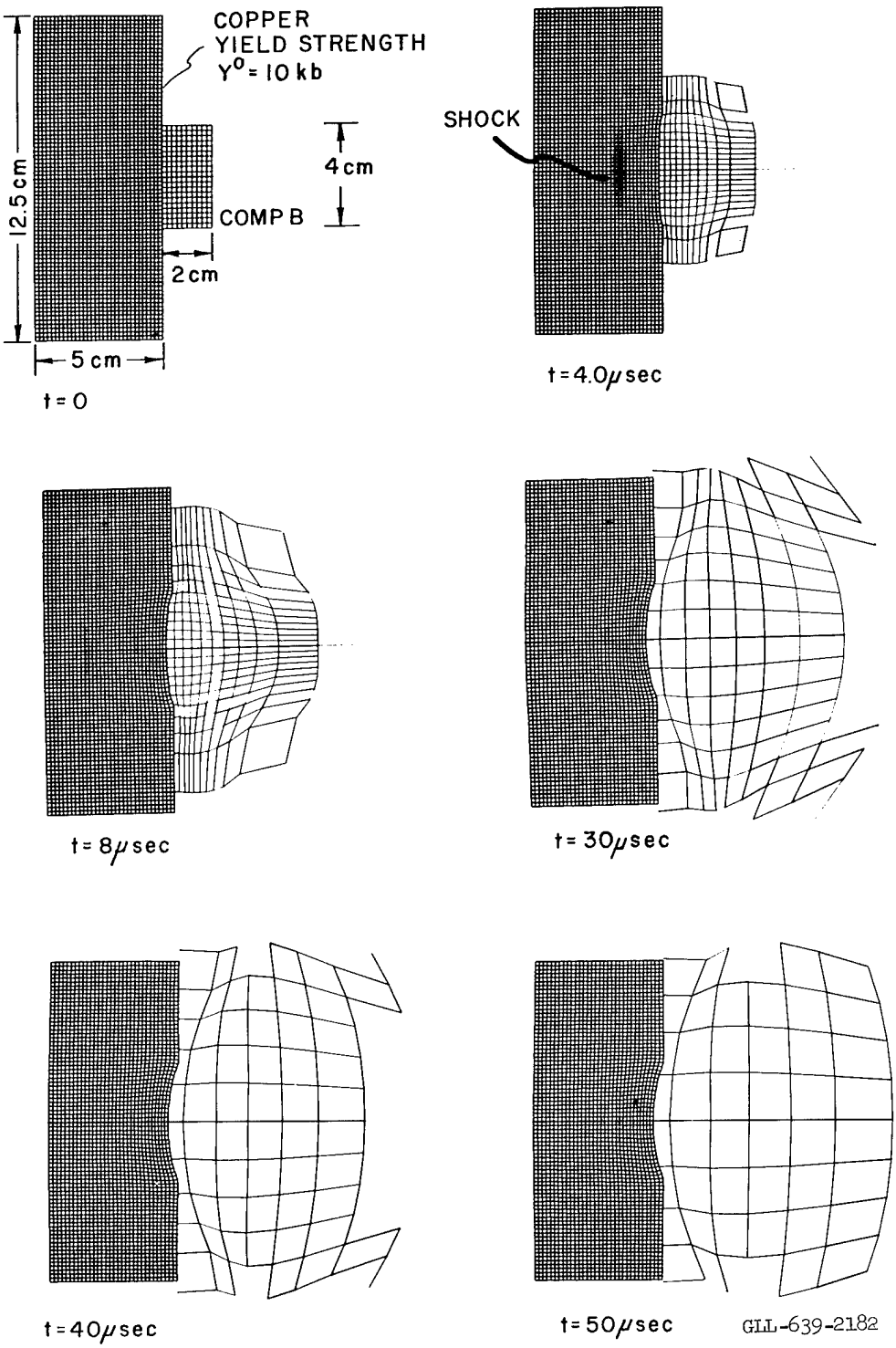

Fig. 8. High-explosive burned at constant volume in contact with a copper plate.

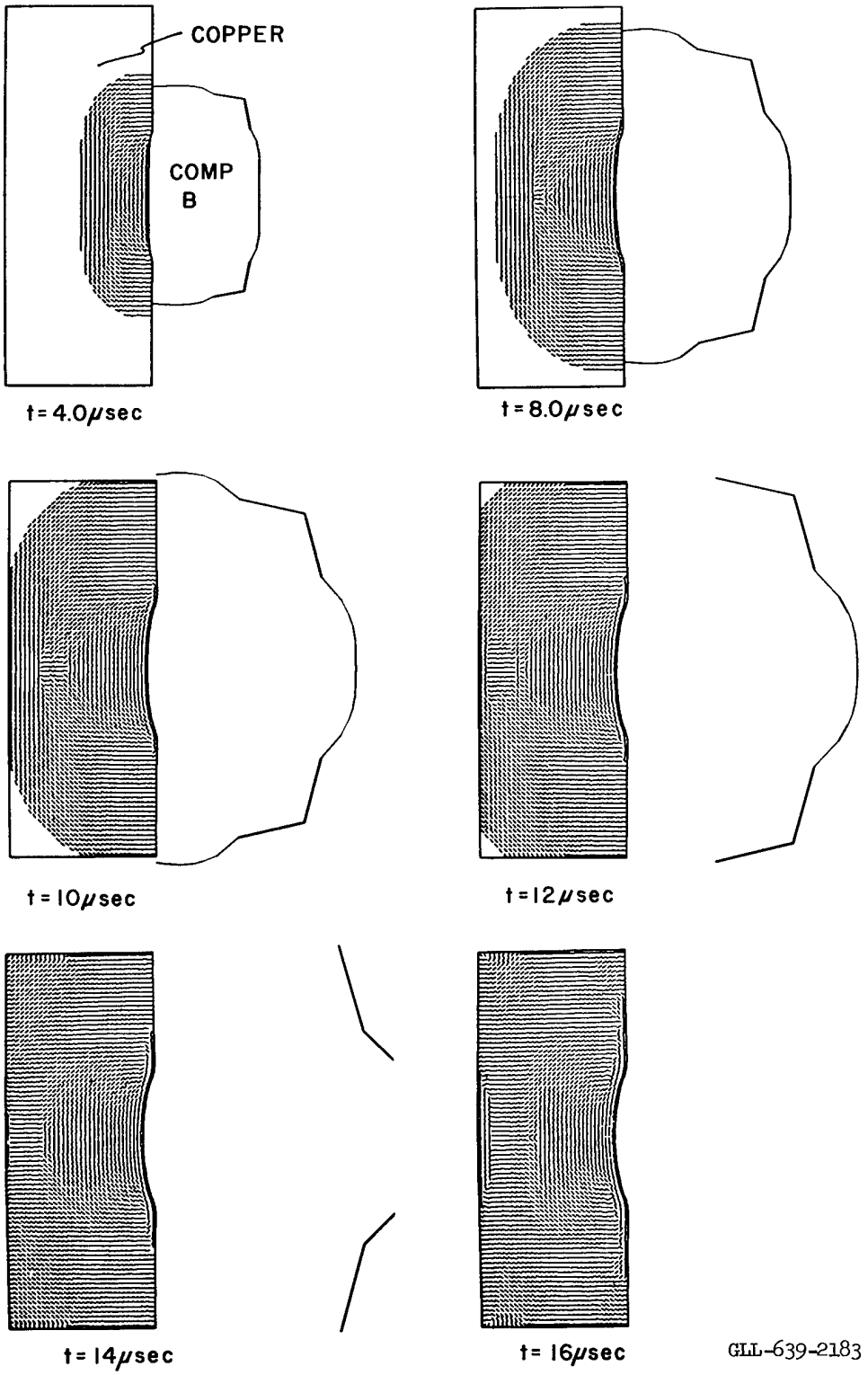

Fig. 9. Direction of the maximum principal stress (see Fig. 8).

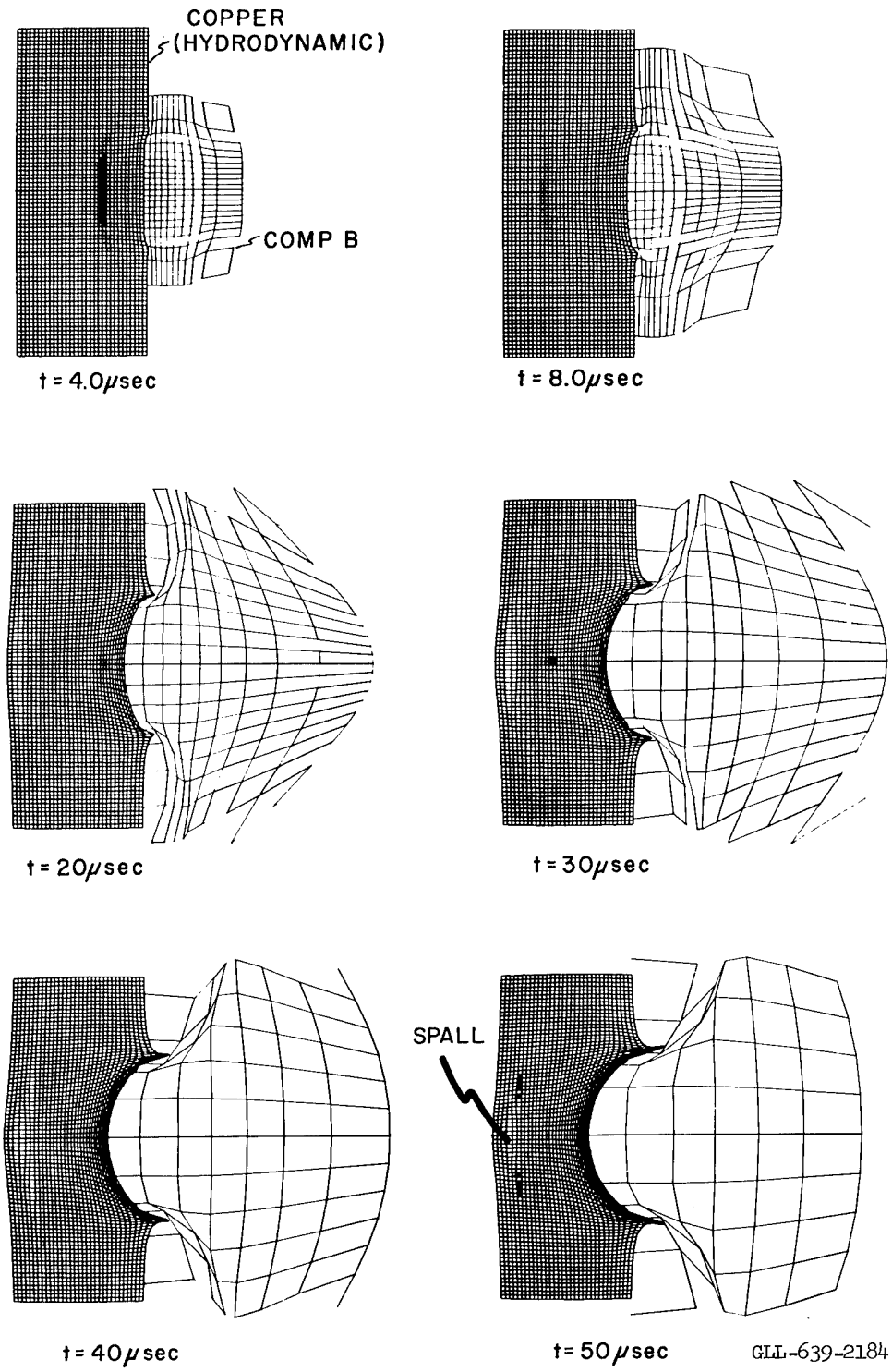

Fig. 10. Initial geometry as in Fig. 8, but with no strength of material in the copper.

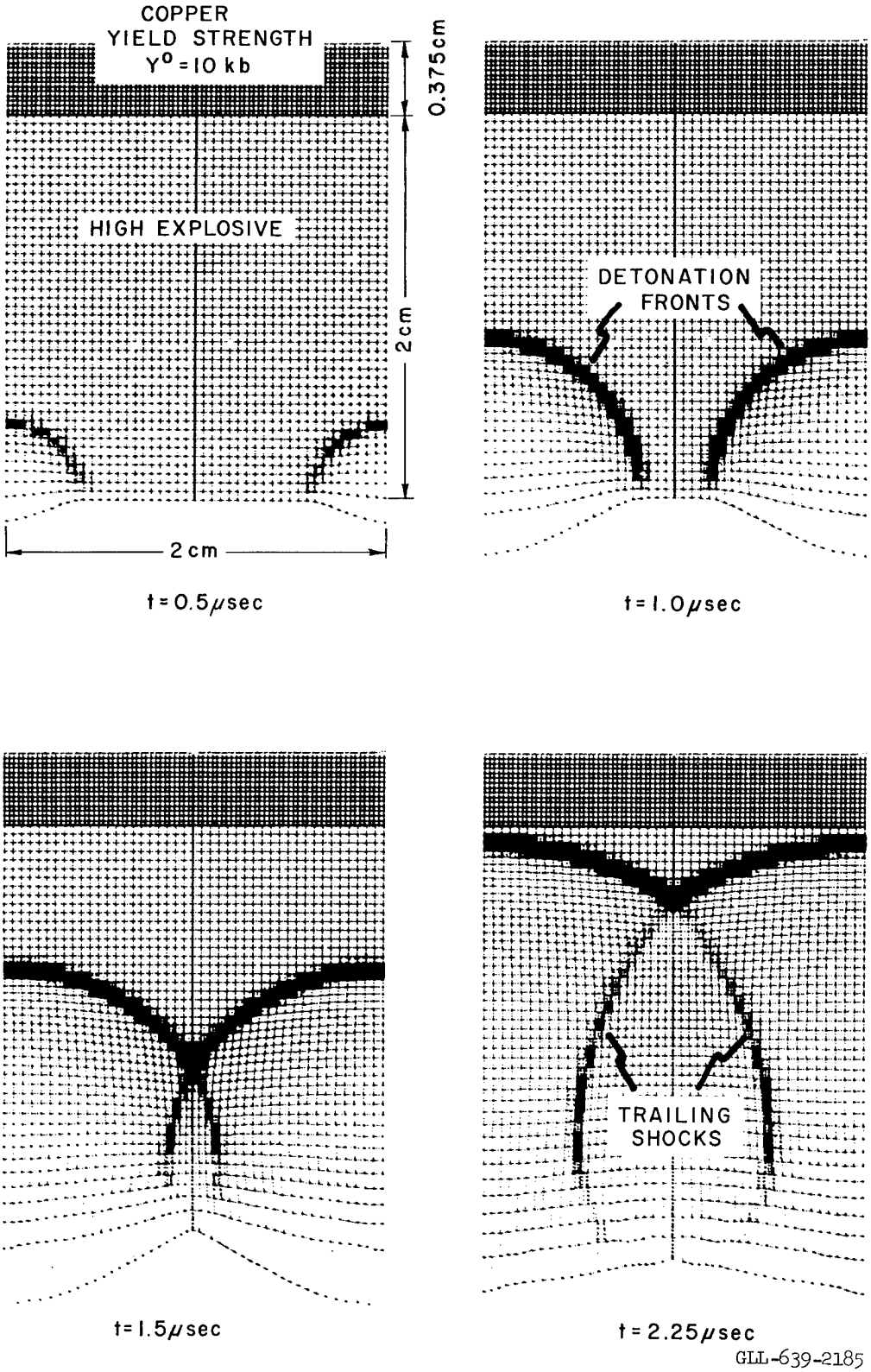

Fig. 11. Stresses induced in a copper plate by high-explosive detonations.

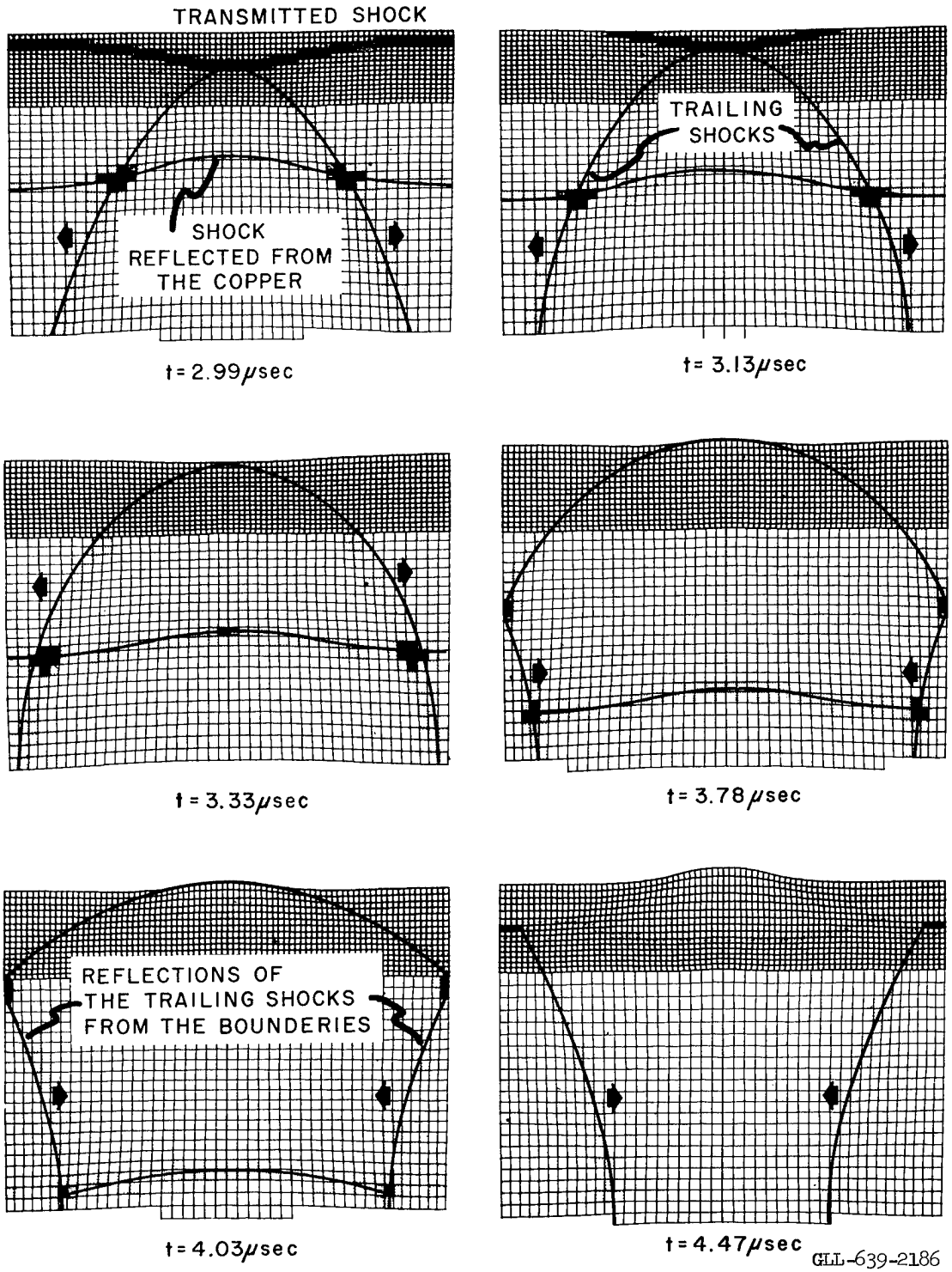

Fig. 12. Continued from Fig. 11.

The interaction of the two detonation fronts results in the trailing shocks with high localized pressures in the region of the cusp. The detonation front can be seen to transmit a shock into the copper and reflect a shock into the high explosive. The trailing shocks induce a circular shock that sweeps from the left and right of the line of interaction. This shock can be seen to punch out the center of the copper. In the last frames the reflection of the trailing shock from the fixed boundaries can be seen. The dark shading where the reflected shock from the copper meets the trailing shocks indicate a high-pressure region.

Figure 13 shows the directions of the maximum principal stresses in the copper for the above problem. The expanding circular shock due to the trailing shocks can be seen to be progressing through the already shocked copper.

Figure 14 shows a comparison of the above problem with a calculation made with no material strength in the copper. This calculation indicates a low density region along the front surface as well as in the large circular section in the middle.

Figure 15 shows the explosion of an iron cylinder that had a charge of PBX 9404 inside that was detonated from the right-hand surface. On the left, the iron cylinder motion has been calculated with no strength of material and on the right, the motion was calculated with a yield strength $Y^0 = 10$ kb. Comparing the two calculations, it can be seen that the elastic-plastic version shows the thickness of the iron to be slightly dilated. Also, the end of the cylinder has maintained more of its original shape compared to the hydrodynamic version.

ACKNOWLEDGMENTS

It is a pleasure to acknowledge the advice and encouragement of Dr. Robert Banaugh and several helpful conversations with Dr. Seymour Sack.

Also, the success of the programs developed here is in a large part due to the programming skills of Dick Giroux for the two-dimensional problem, and John French for the one-dimensional problem.

This work was performed under the auspices of the U. S. Atomic Energy Commission.

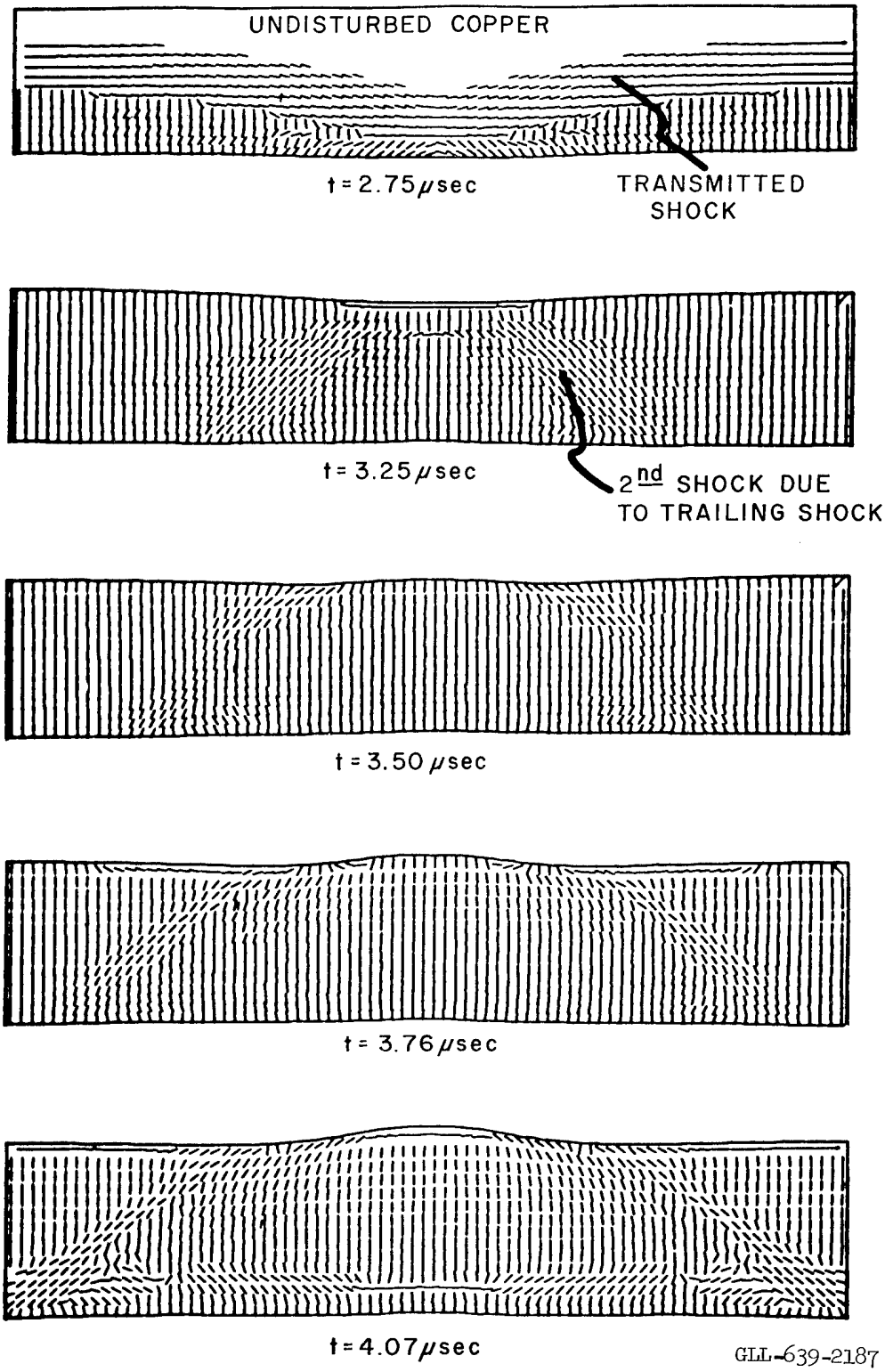

Fig. 13. Direction of the maximum principal stress (see Figs. 11 - 12).

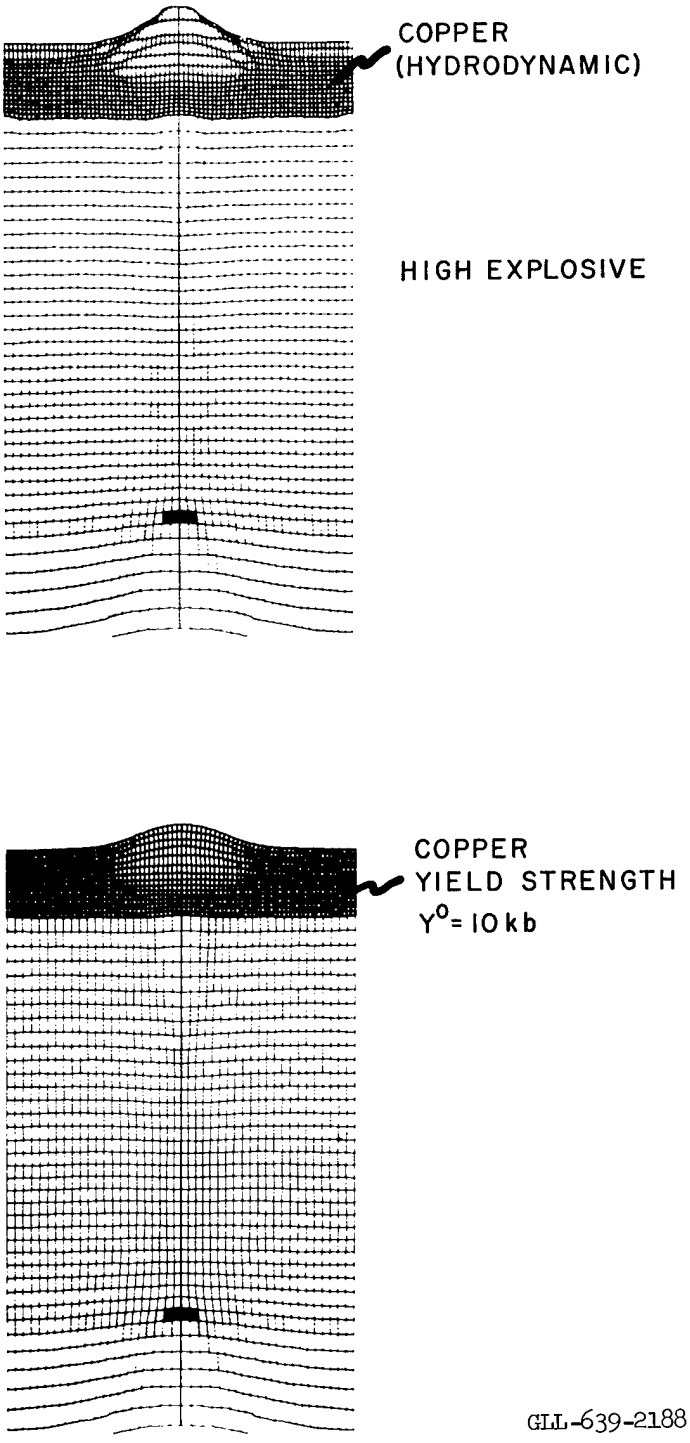

Fig. 14. Comparison at 6 μs with and without material strength.

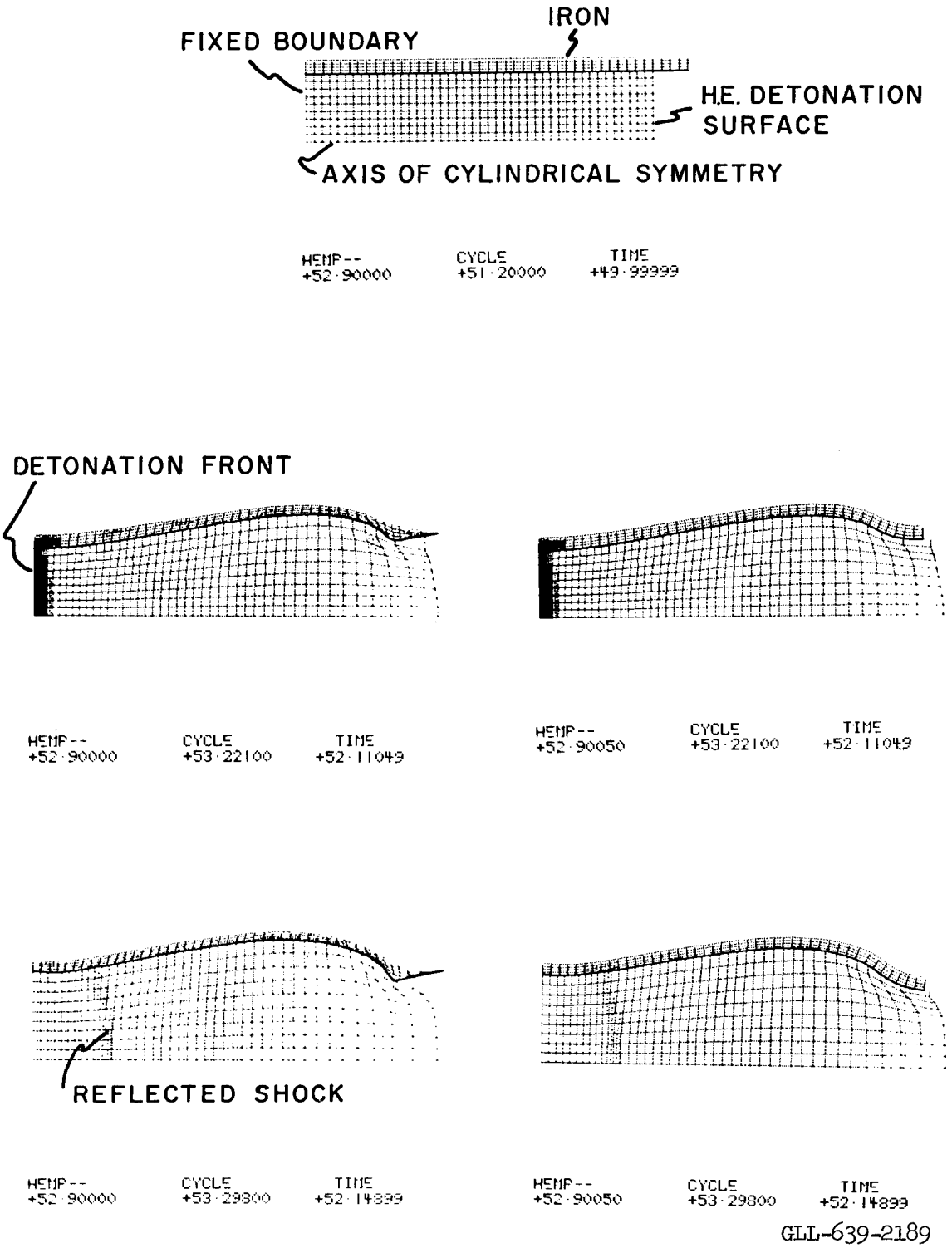

Fig. 15. High-explosive detonated inside of an iron cylinder. (left: Iron treated as a hydrodynamic material; right: Iron treated as an elastic-plastic material with a yield strength $Y^0 = 0.010$ mb).

REFERENCES

[1]William Prager and P. G. Hodge, Theory of Perfectly Plastic Solids (John Wiley and Sons, New York, 1951).

[2]S. Timoshenko, Theory of Elasticity (McGraw-Hill Book Co., Inc., New York, 1951).

[3]L. W. Morland, Phil. Trans. Roy. Soc. A251 341-383 (1959).

[4]R. Von Mises: Zeitchrift fur Angewandte Mathematik und Mechanik v. 8 (1928) English translation: UCRL Trans 872 (L).

[5]A. Nadai, Theory of Flow and Fracture of Solids (McGraw-Hill Book Co., Inc., New York, 1950).

[6]D. C. Drucker, A Definition of Stable Inelastic Material, Journal of Applied Mechanics, March 1959 pages 101-106.

[7]George Duvall, Appl. Mech. Rev., 15 849-854 (1962).

[8]L. V. Al'Tshuler, S. B. Kormer, M. I. Brazhnik, L. A. Vladimirov, M. P. Speranskaya, and A. I. Funtikov. Soviet Physics JETP, 11 No. 4 (October 1960).

[9]John M. Walsh, Melvin H. Rice, Robert G. McQueen, and Frederick L. Yarger, Phys. Rev., 108 No. 2 (1957).

[10]C. D. Lundergan, The Hugoniot Equation of State of 6061-T6 Aluminum at Low Pressures, SC-4637 (RR) (1961).

[11]M. L. Wilkins, Calcul de Detonations Mono et Bidimensionnelles, "Les Ondes de Detonation" Proceedings of colloquium held at Gif-sur-Yvette, France, Aug 28 Sept 2, 1961; Editions du Centre National de la Recherche Scientifique, 15, Quai Anatole-France, Paris (VII^{e}), 1962 pp. 165-175.

[12]F. Wecken and L. Muecke, Detonation d'une charge sphérique, Laboratoire de Rèchercherches Techniques de Saint-Louis Rapports No 8/50 et No 1/53.

[13]M. Reiner, Twelve Lectures on Theoretical Rheology, North Holland Publishing Co. (1949).

[14]G. Maenchen and J. Nuckolls, Paper J, UCRL-6438 Part II.

REFERENCES (Continued)

[15]Reddick & Miller, Advanced Mathematics for Engineers, Second Ed. (John Wiley & Sons Inc., New York, 1947).

[16]R. D. Richtmyer, Difference Methods for Initial Value Problems, Interscience Tracts in Pure and Applied Math No. 4.

APPENDIX A

FINITE DIFFERENCE EQUATIONS FOR THE EQUATIONS GIVEN IN PART II

The material is divided into mass intervals:

$$m_{j+1/2} = \frac{\rho^0}{V^0}\left(\frac{\left(r^0_{j+1}\right)^d - \left(r^0_j\right)^d}{d}\right) \qquad \begin{array}{ll} \text{plane:} & d = 1 \\ \text{cylinderical:} & d = 2 \\ \text{spherical:} & d = 3 \end{array}$$

$j = 1, 2, \ldots N$ (see Ref. 16).

1. Equation of motion

(a) $$U^{n+1/2}_j = U^{n-1/2}_j + \frac{\Delta t^n}{\phi^n_j}\left[\left(\Sigma_r\right)^n_{j+1/2} - \left(\Sigma_r\right)^n_{j-1/2}\right] + \Delta t^n\left(\beta^n_j\right)(d-1)$$

where:

$$\left(\Sigma^n_r\right)_{j+1/2} = \left\{-\left(P^n + q^{n-1/2}\right) + s^n_1\right\}_{j+1/2}$$

$$\left(\Sigma^n_\theta\right)_{j+1/2} = \left\{-\left(P^n + q^{n-1/2}\right) + s^n_2\right\}_{j+1/2}$$

$$\phi_j{}^n = \frac{1}{2}\left[\rho^0_{j+1/2}\left(\frac{r^n_{j+1} - r^n_j}{V^n_{j+1/2}}\right) + \rho^0_{j-1/2}\left(\frac{r^n_j - r^n_{j-1}}{V^n_{j-1/2}}\right)\right]$$

$$\beta^n_j = \frac{1}{2}\left\{\left[\frac{\left(\Sigma_r\right)^n_{j+1/2} - \left(\Sigma_\theta\right)^n_{j+1/2}}{\frac{1}{2}\left(r^n_{j+1} + r^n_j\right)}\right]\left(\frac{V^n}{\rho^0}\right)_{j+1/2} + \left[\frac{\left(\Sigma_r\right)^n_{j-1/2} - \left(\Sigma_\theta\right)^n_{j-1/2}}{\frac{1}{2}\left(r^n_j + r^n_{j-1}\right)}\right]\left(\frac{V^n}{\rho_0}\right)_{j-1/2}\right\}.$$

At an outside regional boundary J

$$\phi^n_J = \rho^0_{J-1/2}\left(\frac{r^n_J - r^n_{J-1}}{V^n_{J-1/2}}\right)\frac{1}{2}$$

$$\beta^n_J = \left[\frac{\left(\Sigma_r\right)^n_{J-1/2} - \left(\Sigma_\theta\right)^n_{J-1/2}}{\frac{1}{2}\left(r^n_J + r^n_{J-1}\right)}\right]\left(\frac{V^n}{\rho_0}\right)_{J-1/2}.$$

At an inside regional boundary J

$$\phi_J^n = \frac{1}{2}\rho^0_{J+1/2}\left(\frac{r^n_{J+1} - r^n_J}{V^n_{J+1/2}}\right)$$

$$\beta_J^n = \left[\frac{(\Sigma_r)^n_{J+1/2} - (\Sigma_\theta)^n_{J+1/2}}{\frac{1}{2}\left(r^n_J + r^n_{J+1}\right)}\right]\left(\frac{V^n}{\rho_0}\right)_{J+1/2}.$$

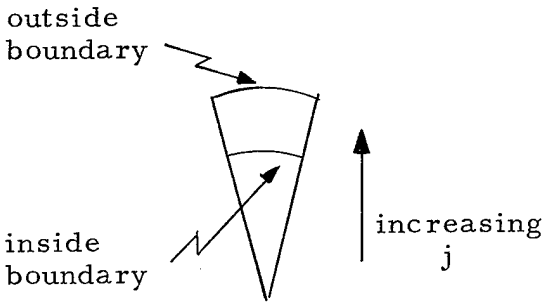

For a free surface at j = J, the stresses are set to zero at J + 1/2 for an outside free surface or J - 1/2 for an inside free surface. The zones adjacent to an elastic region are considered to be hydrodynamic.

(b) $r_j^{n+1} = r_j^n + U_j^{n+1/2}\,\Delta t^{n+1/2}$.

2. Equation of continuity

(a) $$V^{n+1}_{j+1/2} = V^n_{j+1/2} + \Delta t^{n+1/2}\left(\frac{\rho^0}{m}\right)_{j+1/2}\left[U^{n+1/2}_{j+1}\left(r^{n+1/2}_{j+1}\right)^{d-1} - U^{n+1/2}_j\left(r^{n+1/2}_j\right)^{d-1} + \left(\chi^{n+1/2}_{j+1/2}\right)^*\right]$$

(b) $$\eta^{n+1}_{j+1/2} = \frac{1}{V^{n+1}_{j+1/2}} \qquad \text{here } r^{n+1/2}_{j+1} = \frac{1}{2}\left(r^{n+1}_{j+1} + r^n_{j+1}\right) \text{ etc.}$$

$$\left(\chi_{j+1/2}\right)^* = \frac{(\Delta t^{n+1/2})^2}{12}\left[\left(U^{n+1/2}_{j+1}\right)^3 - \left(U^{n+1/2}_j\right)^3\right]$$

3. Anisotropic stresses

velocity strains

$$\left(\dot{\epsilon}_1\right)^{n+1/2}_{j+1/2} = \frac{U^{n+1/2}_{j+1} - U^{n+1/2}_j}{r^{n+1/2}_{j+1} - r^{n+1/2}_j}$$

$$\left(\dot{\epsilon}_2\right)^{n+1/2}_{j+1/2} = \frac{U^{n+1/2}_{j+1} + U^{n+1/2}_j}{r^{n+1/2}_{j+1} + r^{n+1/2}_j}$$

$\dot{\epsilon}_2 = 0$ for d = 1

*Correction term for d = 3 only

$$\text{stress deviators} \begin{cases} \left(s_1\right)^{n+1}_{j+1/2} = \left(s_1\right)^{n}_{j+1/2} + 2\mu\left[\left(\dot{\epsilon}_1\right)^{n+1/2}_{j+1/2}\Delta t^{n+1/2} - \frac{1}{3}\left(\frac{V^{n+1} - V^{n}}{V^{n+1/2}}\right)_{j+1/2}\right] \\ \left(s_2\right)^{n+1}_{j+1/2} = \left(s_2\right)^{n}_{j+1/2} + 2\mu\left[\left(\dot{\epsilon}_2\right)^{n+1/2}_{j+1/2}\Delta t^{n+1/2} - \frac{1}{3}\left(\frac{V^{n+1} - V^{n}}{V^{n+1/2}}\right)_{j+1/2}\right] \\ \left(s_3\right)^{n+1}_{j+1/2} = -\left[\left(s_1\right)^{n+1}_{j+1/2} + \left(s_2\right)^{n+1}_{j+1/2}\right] . \end{cases}$$

4. Artificial viscosity

$q^{n+1/2}_{j+1/2} = C^0\, a\, \rho_0\, \eta^{n+1/2}_{j+1/2} \left| U^{n+1/2}_{j+1} - U^{n+1/2}_{j} \right|$ calculate only if: $U^{n+1/2}_{j+1} < U^{n+1/2}_{j}$

C^0 = constant $\approx 1/2$ and: $\left(V^{n+1}_{j+1/2} - V^{n}_{j+1/2}\right) < 0$.

a = local sound speed

5. Energy equation

$$dE = dE_H + dE_1 + dE_2$$

$$dE_H = -(P + q)\, dV$$

$$dE_1 = V\, s_1 \dot{\epsilon}_1 \Delta t$$

$$dE_2 = V\, s_2 \dot{\epsilon}_2 \Delta t\, (d-1)$$

(a) $$\left(E_1\right)^{n+1}_{j+1/2} = \left(E_1\right)^{n}_{j+1/2} + V^{n+1/2}_{j+1/2}\left(s_1\right)^{n+1/2}_{j+1/2}\left(\dot{\epsilon}_1\right)^{n+1/2}_{j+1/2}\Delta t^{n+1/2}$$

(b) $$\left(E_2\right)^{n+1}_{j+1/2} = \left(E_2\right)^{n}_{j+1/2} + (d-1)V^{n+1/2}_{j+1/2}\left(s_2\right)^{n+1/2}_{j+1/2}\left(\dot{\epsilon}_2\right)^{n+1/2}_{j+1/2}\Delta t^{n+1/2}$$

(c) $$\left(E\right)^{n+1}_{j+1/2} = \left\{\frac{E^{n} - \left[\frac{A(\eta^{n+1}) + P^{n}}{2} + q^{n+1/2}\right]\cdot\left[V^{n+1} - V^{n}\right] + dE_1 + dE_2}{1 + \frac{B(\eta^{n+1})}{2}\cdot\left[V^{n+1} - V^{n}\right]}\right\}_{j+1/2} .$$

6. Hydrostatic pressure

$$P_{j+1/2}^{n+1} = A\left(\eta_{j+1/2}^{n+1}\right) + B\left(\eta_{j+1/2}^{n+1}\right) E_{j+1/2}^{n+1} .$$

7. Von Mises yield condition

$$\left(s_1^2 + s_2^2 + s_3^2\right)^{n+1} - 2/3\,(Y^0)^2 = K^{n+1}$$

If $K^{n+1} \leq 0$, the material element is within the elastic limit.

If $K^{n+1} > 0$, the material element is beyond the elastic limit.

Set:
$$\begin{cases} s_1^{n+1} = s_1^{n+1}\sqrt{2/3}\cdot Y^0 \Big/ \sqrt{s_1^2 + s_2^2 + s_3^2} \\ s_2^{n+1} = s_2^{n+1}\sqrt{2/3}\cdot Y^0 \Big/ \sqrt{s_1^2 + s_2^2 + s_3^2} \end{cases} .$$

8. Stability

$$\Delta t^{n+3/2} = \frac{1}{3}\left.\frac{r_{j+1}^{n+1} - r_j^{n+1}}{\sqrt{a^2 + b^2}}\right|_{\text{min. over } j}$$

If: $\Delta t^{n+3/2} > (1.1)\Delta t^{n+1/2}$

a = sound speed

b = $(2C^0)\frac{\dot{V}}{V}$; b = 0 if $\frac{\dot{V}}{V} \geq 0$

Use: $\Delta t^{n+3/2} = (1.1)\Delta t^{n+1/2}$

$$\Delta t^{n+1} = \frac{1}{2}\left(\Delta t^{n+3/2} + \Delta t^{n+1/2}\right) .$$

This is a composite of the stability criteria given in the Von Neumann and Richtmyer paper that introduced the "q" method for calculating shocks (J. Appl. Phys. 21, March 1950).

APPENDIX B

FINITE DIFFERENCE EQUATIONS FOR THE EQUATIONS GIVEN IN PART III

1. Mass zoning for cylindrical symmetry about the x-axis.

The material is divided into quadrilaterals with a grid j-k that moves with the material. In the figure, the centers and the vertices of the quadrilaterals will be denoted as follows:

$① \equiv j + \frac{1}{2},\ k + \frac{1}{2} \qquad 1 \equiv j, k$

$② \equiv j - \frac{1}{2},\ k + \frac{1}{2} \qquad 2 \equiv j + 1, k$

$③ \equiv j - \frac{1}{2},\ k - \frac{1}{2} \qquad 3 \equiv j + 1, k + 1$

$④ \equiv j + \frac{1}{2},\ k - \frac{1}{2} \qquad 4 \equiv j, k + 1$

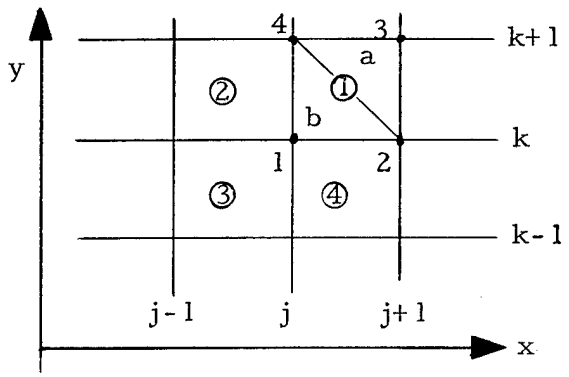

The mass at time zero associated with each quadrilateral is obtained by the product of the initial density and the volume swept out by the quadrilateral rotated about the x-axes. For example, the mass at time zero for quadrilateral ① is calculated as follows:

$$(a)\quad M_{①} = \frac{1}{3}\left(\frac{\rho^0}{V^0}\right)_{①}\left[\left(y_2^{\,0} + y_3^{\,0} + y_4^{\,0}\right) A_a^{\,0} + \left(y_1^{\,0} + y_2^{\,0} + y_4^{\,0}\right) A_b^{\,0}\right]_{①};$$

masses $M_{②}$, $M_{③}$, and $M_{④}$ are calculated similarly.

A_a = area of Δa; A_b = area of Δb:

$$(b)\quad \begin{cases} \left(A_a\right)_{①}^{n} = \frac{1}{2}\left[x_2^{\,n}\left(y_3^{\,n} - y_4^{\,n}\right) + x_3^{\,n}\left(y_4^{\,n} - y_2^{\,n}\right) + x_4^{\,n}\left(y_2^{\,n} - y_3^{\,n}\right)\right], \\ \left(A_b\right)_{①}^{n} = \frac{1}{2}\left[x_2^{\,n}\left(y_4^{\,n} - y_1^{\,n}\right) + x_4^{\,n}\left(y_1^{\,n} - y_2^{\,n}\right) + x_1^{\,n}\left(y_2^{\,n} - y_4^{\,n}\right)\right], \\ A_{①}^{\,n} = \left(A_a\right)_{①}^{n} + \left(A_b\right)_{①}^{n}. \end{cases}$$

2. Conservation of mass

$$V_{①}^{\,n} = \frac{1}{3}\left(\frac{\rho^0}{M}\right)_{①}\left[\left(y_2^{\,n} + y_3^{\,n} + y_4^{\,n}\right) A_a^{\,n} + \left(y_1^{\,n} + y_2^{\,n} + y_4^{\,n}\right) A_b^{\,n}\right]_{①}$$

$$V_{①}^{\,n} = \left(\rho^0/\rho^n\right)_{①}.$$

3. Equations of motion

The equations are centered at point j, k; see figure for notation.

I = j, k - 1

II = j + 1, k

III = j, k + 1

IV = j - 1, k.

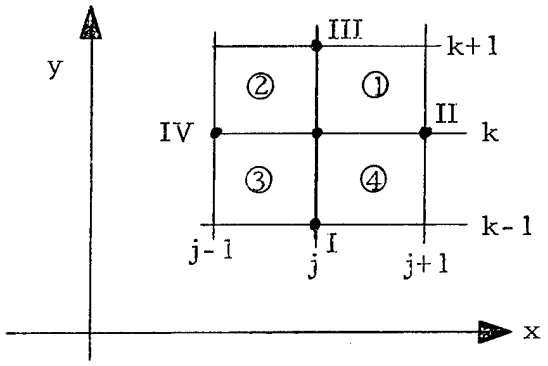

$$(a)\quad \dot{x}^{n+1/2}_{j,k} = \dot{x}^{n-1/2}_{j,k} - \frac{\Delta t^n}{2\phi^n_{j,k}}\left[\left(\Sigma_{xx}\right)^n_{①}\left(y^n_{II} - y^n_{III}\right) + \left(\Sigma_{xx}\right)^n_{②}\left(y^n_{III} - y^n_{IV}\right)\right.$$

$$+\left(\Sigma_{xx}\right)^n_{③}\left(y^n_{IV} - y^n_{I}\right) + \left(\Sigma_{xx}\right)^n_{④}\left(y^n_{I} - y^n_{II}\right) - \left(T_{xy}\right)^n_{①}\left(x^n_{II} - x^n_{III}\right)$$

$$\left. - \left(T_{xy}\right)^n_{②}\left(x^n_{III} - x^n_{IV}\right) - \left(T_{xy}\right)^n_{③}\left(x^n_{IV} - x^n_{I}\right) - \left(T_{xy}\right)^n_{④}\left(x^n_{I} - x^n_{II}\right)\right] + \Delta t^n\,(a)^n_{j,k}.$$

$$(b)\quad \dot{y}^{n+1/2}_{j,k} = \dot{y}^{n-1/2}_{j,k} + \frac{\Delta t^n}{2\phi^n_{j,k}}\left[\left(\Sigma_{yy}\right)^n_{①}\left(x^n_{II} - x^n_{III}\right) + \left(\Sigma_{yy}\right)^n_{②}\left(x^n_{III} - x^n_{IV}\right)\right.$$

$$+\left(\Sigma_{yy}\right)^n_{③}\left(x^n_{IV} - x^n_{I}\right) + \left(\Sigma_{yy}\right)^n_{④}\left(x^n_{I} - x^n_{II}\right) - \left(T_{xy}\right)^n_{①}\left(y^n_{II} - y^n_{III}\right)$$

$$\left. - \left(T_{xy}\right)^n_{②}\left(y^n_{III} - y^n_{IV}\right) - \left(T_{xy}\right)^n_{③}\left(y^n_{IV} - y^n_{II}\right) - \left(T_{xy}\right)^n_{④}\left(y^n_{I} - y^n_{II}\right)\right] + \Delta t^n\,(\beta)^n_{j,k}.$$

$$(c)\quad \phi^n_{j,k} = \frac{1}{4}\left[\left(\frac{\rho^0 A^n}{V^n}\right)_{①} + \left(\frac{\rho^0 A^n}{V^n}\right)_{②} + \left(\frac{\rho^0 A^n}{V^n}\right)_{③} + \left(\frac{\rho^0 A^n}{V^n}\right)_{④}\right],$$

$$a^n_{j,k} = \frac{1}{4}\left\{\left[T_{xy}\left(\frac{A^n}{M}\right)\right]_{①} + \left[T_{xy}\left(\frac{A^n}{M}\right)\right]_{②} + \left[T_{xy}\left(\frac{A^n}{M}\right)\right]_{③} + \left[T_{xy}\left(\frac{A^n}{M}\right)\right]_{④}\right\},$$

$$\beta^n_{j,k} = \frac{1}{4}\left\{\left[\left(\Sigma^n_{yy} - \Sigma^n_{\theta\theta}\right)\left(\frac{A^n}{M}\right)\right]_{①} + \left[\left(\Sigma^n_{yy} - \Sigma^n_{\theta\theta}\right)\left(\frac{A^n}{M}\right)\right]_{②} + \left[\left(\Sigma^n_{yy} - \Sigma^n_{\theta\theta}\right)\left(\frac{A^n}{M}\right)\right]_{③}\right.$$

$$\left. + \left[\left(\Sigma^n_{yy} - \Sigma^n_{\theta\theta}\right)\left(\frac{A^n}{M}\right)\right]_{④}\right\}.$$

(d) $x_{j,k}^{n+1} = x_{j,k}^{n} + \dot{x}_{j,k}^{n+1/2}\,\Delta t^{n+1/2}$,

$y_{j,k}^{n+1} = y_{j,k}^{n} + \dot{y}_{j,k}^{n+1/2}\,\Delta t^{n+1/2}$.

(e) Calculate $V_{①}^{n+1}$ from Eq. (2) (conservation of mass).

(f) Calculate $q_{①}^{n+1/2}$ from the equation of state section.

4. Equation of state

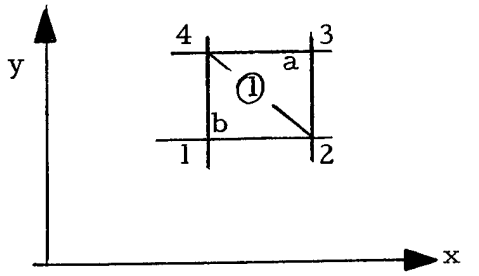

(A) Strains

$$A_{①} \equiv (A_a)_{①} + (A_b)_{①},$$

$$A_{①}^{n+1/2} = \frac{1}{2}\left(A_{①}^{n+1} + A_{①}^{n}\right).$$

(i) $$(\dot{\epsilon}_{xx})_{①}^{n+1/2} = \left(\frac{\partial \dot{x}}{\partial x}\right)_{①}^{n+1/2} = \frac{1}{2A_{①}^{n+1/2}}\left[(\dot{x}_2 - \dot{x}_4)(y_3 - y_1) - (y_2 - y_4)(\dot{x}_3 - \dot{x}_1)\right]^{n+1/2}.$$

(ii) $$(\dot{\epsilon}_{yy})_{①}^{n+1/2} = \left(\frac{\partial \dot{y}}{\partial y}\right)_{①}^{n+1/2} = \frac{-1}{2A_{①}^{n+1/2}}\left[(\dot{y}_2 - \dot{y}_4)(x_3 - x_1) - (x_2 - x_4)(\dot{y}_3 - \dot{y}_1)\right]^{n+1/2}.$$

(iii) $$(\dot{\epsilon}_{\theta\theta})^{n+1/2} = \left(\frac{\dot{y}}{y}\right)_{①}^{n+1/2} = \left[\frac{\dot{V}}{V} - (\dot{\epsilon}_{xx} + \dot{\epsilon}_{yy})\right]_{①}.$$

(iv) $$(\dot{\epsilon}_{xy})_{①}^{n+1/2} = \left(\frac{\partial \dot{y}}{\partial x} + \frac{\partial \dot{x}}{\partial y}\right)_{①}^{n+1/2}$$

$$= \frac{1}{2A_{①}^{n+1/2}}\left\{\left[(\dot{y}_2 - \dot{y}_4)(y_3 - y_1) - (y_2 - y_4)(\dot{y}_3 - \dot{y}_1)\right] - \left[(\dot{x}_2 - \dot{x}_4)(x_3 - x_1) - (x_2 - x_4)(\dot{x}_3 - \dot{x}_1)\right]\right\}^{n+1/2}.$$

(v) $$\left(\Delta\epsilon_{xx}\right)_{①}^{n+1/2} = \left(\dot{\epsilon}_{xx}\right)_{①}^{n+1/2}\Delta t^{n+1/2}$$

$$\left(\Delta\epsilon_{yy}\right)_{①}^{n+1/2} = \left(\dot{\epsilon}_{yy}\right)_{①}^{n+1/2}\Delta t^{n+1/2}$$

$$\left(\Delta\epsilon_{\theta\theta}\right)_{①}^{n+1/2} = \left(\dot{\epsilon}_{\theta\theta}\right)_{①}^{n+1/2}\Delta t^{n+1/2}$$

$$\left(\Delta\epsilon_{xy}\right)_{①}^{n+1/2} = \left(\dot{\epsilon}_{xy}\right)_{①}^{n+1/2}\Delta t^{n+1/2}$$

$$\left(\frac{\Delta V}{V}\right)_{①}^{n+1/2} = \frac{\dot{V}_{①}}{V_1}\Delta t^{n+1/2} = \frac{V_{①}^{n+1} - V_{①}^{n}}{V_{①}^{n+1/2}}$$

where

$$V_{①}^{n+1/2} = \frac{1}{2}\left(V_{①}^{n+1} + V_{①}^{n}\right).$$

(B) Stresses

1. Elastic

(i) $$\left(s_{xx}\right)_{①}^{n+1} = \left(s_{xx}\right)_{①}^{n} + 2\mu\left[\Delta\epsilon_{xx}^{n+1/2} - \frac{1}{3}\left(\frac{\Delta V}{V}\right)^{n+1/2}\right]_{①} + \left(\delta_{xx}\right)_{①}^{n}$$

(ii) $$\left(s_{yy}\right)_{①}^{n+1} = \left(s_{yy}\right)_{①}^{n} + 2\mu\left[\Delta\epsilon_{yy}^{n+1/2} - \frac{1}{3}\left(\frac{\Delta V}{V}\right)^{n+1/2}\right]_{①} + \left(\delta_{yy}\right)_{①}^{n}$$

(iii) $$\left(s_{\theta\theta}\right)_{①}^{n+1} = \left(s_{\theta\theta}\right)_{①}^{n} + 2\mu\left[\Delta\epsilon_{\theta\theta}^{n+1/2} - \frac{1}{3}\left(\frac{\Delta V}{V}\right)^{n+1/2}\right]_{①}$$

(iv) $$\left(T_{xy}\right)_{①}^{n+1} = \left(T_{xy}\right)_{①}^{n} + \mu\left(\Delta\epsilon_{xy}^{n+1/2}\right)_{①} + \left(\delta_{xy}\right)_{①}^{n}.$$

See Section 6 for the calculation of δ_{xx}, δ_{yy}, and δ_{xy}. After the stresses at time t^{n+1} are calculated, the yield calculations are made (see Section 7).

2. Hydrodynamic

$$P_{①}^{n+1} = A\left(V_{①}^{n+1}\right) + B\left(V_{①}^{n+1}\right) \cdot E_{①}^{n+1}.$$

$E_{①}^{n+1}$ is calculated from the total internal energy equation, Section 5.

3. Artificial viscosity

(i) quadratic q: $$q_{①}^{n+1/2} = \left[\frac{C_0^2 \rho^0 A^{n+1/2}}{V^{n+1/2}} \cdot \left(\frac{\dot{V}}{V}\right)^2\right]_{①}$$

$C_0^2 = 4.$ Calculate only for $\dot{V}/V < 0.$

(ii) linear q: $$q_{①}^{n+1/2} = \left(\frac{aC_L \rho^0 \sqrt{A^{n+1/2}}}{V^{n+1/2}}\left|\frac{\dot{V}}{V}\right|\right)_{①}$$

C_L = constant. Calculate only for $\dot{V}/V < 0.$

a = sound speed.

(iii) anisotropic q:
$$\begin{cases} \left(q_{xx}\right)^{n+1/2}_{①} = \left[\dfrac{aC_A\rho\sqrt{0(A^{n+1/2})}}{V^{n+1/2}}\dot{\epsilon}_{xx}\right]① , \\ \left(q_{yy}\right)^{n+1/2}_{①} = \left[\dfrac{aC_A\rho\sqrt{0(A^{n+1/2})}}{V^{n+1/2}}\dot{\epsilon}_{yy}\right]① \\ C_A = \text{constant.} \end{cases}$$

If these terms are used, they are added to the appropriate stresses, i.e., $(s_{xx} + q_{xx})$ and $(s_{yy} + q_{yy})$. It is useful to have the q formulated in this way for problems where a shock is travelling perpendicular to a free surface. However, for the average problem the quadratic q gives very satisfactory results and it is this q that is expressed in the equations written here.

4. Total stresses

(i) $\left[\Sigma_{xx}\right]^{n+1}_{①} = \left[s_{xx}\right]^{n+1}_{①} - \left[P^{n+1} + q^{n+1/2}\right]_{①}$.

(ii) $\left[\Sigma_{yy}\right]^{n+1}_{①} = \left[s_{yy}\right]^{n+1}_{①} - \left[P^{n+1} + q^{n+1/2}\right]_{①}$.

(iii) $\left[\Sigma_{\theta\theta}\right]^{n+1}_{①} = \left[s_{\theta\theta}\right]^{n+1}_{①} - \left[P^{n+1} + q^{n+1/2}\right]_{①}$.

5. Energy equations

(i) total internal:

$$E^{n+1}_{①} = \left\{\frac{E^n - \left[\dfrac{A(V^{n+1}) + P^n}{2} + q^{n+1/2}\right]\cdot (V^{n+1} - V^n) + \Delta Z^{n+1/2}}{1 + \dfrac{B(V^{n+1})}{2}(V^{n+1} - V^n)}\right\}_{①}$$

(ii) anisotropic:
$$Z^{n+1}_{①} = Z^n{}_{①} + V^{n+1/2}_{①}\cdot\left\{s_{xx}\epsilon_{xx} + s_{yy}\epsilon_{yy} + s_{\theta\theta}\epsilon_{\theta\theta} + T_{xy}\epsilon_{xy}\right\}^{n+1/2}_{①}$$

$$\Delta Z^{n+1/2} = Z^{n+1} - Z^n;\ s^{n+1/2} = \frac{1}{2}(s^{n+1} + s^n),\ \text{etc.}$$

6. Correction for rotation of stresses during a time step $\Delta t^{n+1/2}$.

If a mass element has rotated in the x-y plane by angle ω during the time interval $\Delta t^{n+1/2} = t^{n+1} - t^n$, the stresses must be recalculated so that they will be referred to the x-y coordinate system in their new position.

The following transformation equations can be obtained from Ref. 2, p. 14:

$$\text{(i)} \quad \begin{cases} s'_{xx} = s^n_{xx} \cos^2 \omega + s^n_{yy} \sin^2 \omega + 2T^n_{xy} \sin \omega \cos \omega \\ s'_{yy} = s^n_{xx} \sin^2 \omega + s^n_{yy} \cos^2 \omega - 2T^n_{xy} \sin \omega \cos \omega \\ T'_{xy} = T^n_{xy} \left[\cos^2 \omega - \sin^2 \omega\right] - \left[s^n_{xx} - s^n_{yy}\right] \cos \omega \sin \omega . \end{cases}$$

The angle ω is given by:

$$\text{(ii)} \quad \nabla x \, (\dot{x}\hat{i} - \dot{y}\hat{j}) = \left(\frac{\partial \dot{y}}{\partial x} - \frac{\partial \dot{x}}{\partial y}\right)\hat{k} = 2 \sin \dot{\omega}$$

$$\sin \omega = \frac{\Delta t^{n+1/2}}{2} \left(\frac{\partial \dot{y}}{\partial x} - \frac{\partial \dot{x}}{\partial y}\right) .$$

Equations (i) can be rewritten as:

$$\text{(iii)} \quad \begin{cases} s'_{xx} = \dfrac{s^n_{xx} + s^n_{yy}}{2} + \dfrac{s^n_{xx} - s^n_{yy}}{2} \cos 2\omega + T^n_{xy} \sin 2\omega \\ s'_{yy} = \dfrac{s^n_{xx} + s^n_{yy}}{2} - \dfrac{s^n_{xx} - s^n_{yy}}{2} \cos 2\omega - T^n_{xy} \sin 2\omega \\ T'_{xy} = T^n_{xy} \cos 2\omega - \dfrac{s^n_{xx} - s^n_{yy}}{2} \sin 2\omega . \end{cases}$$

In the incremental stress-strain relations:

$$\text{(iv)} \quad s^{n+1}_{xx} = s^n_{xx} + 2\mu\left[\epsilon_{xx} - \frac{1}{3}\frac{\Delta V}{V}\right]^{n+1/2}, \text{ etc.},$$

the stresses s^n_{xx}, s^n_{yy}, and T^n_{xy} must be replaced by s'_{xx}, s'_{yy}, and T'_{xy}. In order to preserve the form of Eq. (iv), it is convenient to introduce an additive term, δ, to the stresses such that

$$s^{n+1}_{xx} = s^n_{xx} + 2\mu\left[\epsilon_{xx} - \frac{1}{3}\frac{\Delta V}{V}\right]^{n+1/2} + \delta^n_{xx}, \text{ etc.}$$

$$\text{(v)} \quad \begin{cases} \delta^n_{xx} = s'_{xx} - s^n_{xx} = \left(\dfrac{s^n_{xx} - s^n_{yy}}{2}\right)(\cos 2\omega - 1) + T^n_{xy} \sin 2\omega \\ \delta^n_{yy} = s'_{yy} - s^n_{yy} = 1\ \delta^n_x \\ \delta^n_{xy} = T'_{xy} - T^n_{xy} = T^n_{xy} (\cos 2\omega - 1) - \left(\dfrac{s^n_{xx} - s^n_{yy}}{2}\right) \sin 2\omega \\ \sin 2\omega \approx 2 \sin \omega = \left(\dfrac{\partial \dot{y}}{\partial x} - \dfrac{\partial \dot{x}}{\partial y}\right) \Delta t^{n+1/2}. \end{cases}$$

7. Yield calculations

(a) Principal stresses (Ref. 5, p. 94)

(i) $$s_1^{n+1} = \frac{s_{xx}^{n+1} + s_{yy}^{n+1}}{2} + \frac{1}{2}\left[\left(s_{xx}^{n+1} - s_{yy}^{n+1}\right)^2 + \left(2T_{xy}^{n+1}\right)^2\right]^{1/2}$$

(ii) $$s_2^{n+1} = \frac{s_{xx}^{n+1} + s_{yy}^{n+1}}{2} - \frac{1}{2}\left[\left(s_{xx}^{n+1} - s_{yy}^{n+1}\right)^2 + \left(2T_{xy}^{n+1}\right)^2\right]^{1/2}$$

(iii) $$s_3^{n+1} = s_{\theta\theta}^{n+1} .$$

(In the plane x-y and cylindrical coordinate systems used here $s_{\theta\theta}$ is already a principal stress.)

(b) Von Mises yield condition

calculate

(i) $$2J^{n+1} = \left[\left(s_1^{n+1}\right)^2 + \left(s_2^{n+1}\right)^2 + \left(s_3^{n+1}\right)^2\right]$$

$$= \left[\left(s_{xx}^{n+1}\right)^2 + \left(s_{yy}^{n+1}\right)^2 + \left(s_{\theta\theta}^{n+1}\right)^2\right] + 2\left(T_{xy}^{n+1}\right)^2$$

(ii) $$2J^{n+1} - 2/3\,(Y^0)^2 = K^{n+1} .$$

If $K^{n+1} > 0$ then multiply each of the stresses s_{xx}^{n+1}, s_{yy}^{n+1}, $s_{\theta\theta}^{n+1}$, and T_{xy}^{n+1} by $\sqrt{2/3}\, Y^0 \Big/ \sqrt{2J^{n+1}}$. If $K^{n+1} \leq 0$ use the stresses as they are for the next time step.

8. Boundary conditions

(a) Fixed boundary on the x axis

Phantom zones are created by a mirror reflection across the boundary as shown in the figure.

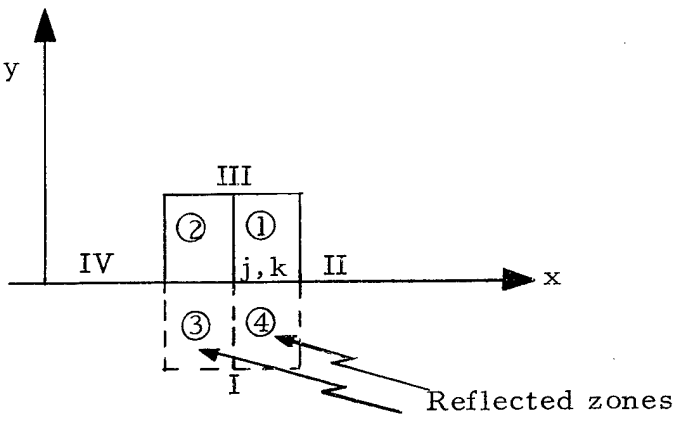

The point j, k can now be accelerated with the equation of motion for a general point [Eqs. (3)] subject to the following conditions:

$$\text{(i)} \quad \begin{cases} \dot{y}_{j,k} = 0 \\ \left(\Sigma^n_{xx}\right)_{④} = \left(\Sigma^n_{xx}\right)_{①} \\ \left(\Sigma^n_{xx}\right)_{③} = \left(\Sigma^n_{xx}\right)_{②} \\ \left(T^n_{xy}\right)_{④} = -\left(T^n_{xy}\right)_{①} \\ \left(T^n_{xy}\right)_{③} = -\left(T^n_{xy}\right)_{②} \\ M_{④} = M_{①} \\ M_{③} = M_{②} \end{cases}$$

The above procedure gives the desired acceleration along the boundary, but is has the undesirable feature of not allowing for the situation when the point j,k is on a free surface since the point has the extra mass of the reflected zones associated with it. It is more convenient to have the correct mass associated with each point, determined once and for all when the problem grid is generated, and use different, acceleration routines for the case when the boundary is fixed. Therefore, referring to the figure above, we will calculate $\phi_{j,k}$ as:

$$\text{(ii)} \qquad \phi^n_{j,k} = \frac{1}{4}\left[\left(\frac{\rho^0 A^n}{V^n}\right)_{①} + \left(\frac{\rho^0 A^n}{V^n}\right)_{②}\right].$$

The acceleration equation for point j,k that gives the same results as the equations of motion for a general point with conditions (i) becomes:

$$\text{(iii)} \qquad (dx/dt)_{j,k} = -\frac{1}{2\phi^n_{j,k}}\left\{\left[\left(\Sigma^n_{xx}\right)_{①} - \left(\Sigma^n_{xx}\right)\right]_{②}\left[y^n_{II} - y^n_{III}\right]\right.$$
$$\left. - \left(T^n_{xy}\right)_{①}\left[x^n_{II} - s^n_{III}\right] - \left(T^n_{xy}\right)_{②}\left[x^n_{III} - x^n_{IV}\right]\right\}.$$

(b) Fixed boundary on the y axis

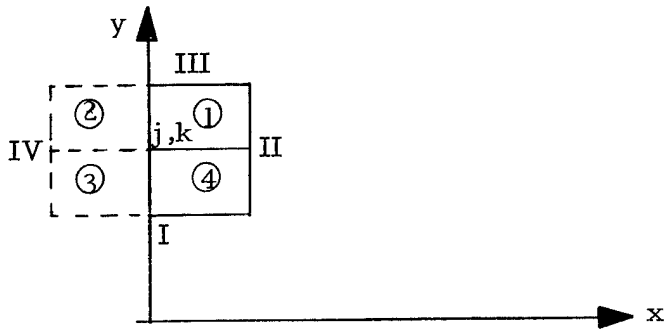

$$
\text{(i)}\quad \begin{cases}
x_{j,k} = 0 \\
\left(\Sigma^n_{yy}\right)_{②} = \left(\Sigma^n_{yy}\right)_{①} \\
\left(\Sigma^n_{yy}\right)_{③} = \left(\Sigma^n_{yy}\right)_{④} \\
\left(\Sigma^n_{\theta\theta}\right)_{②} = \left(\Sigma^n_{\theta\theta}\right)_{①} \\
\left(\Sigma^n_{\theta\theta}\right)_{③} = \left(\Sigma^n_{\theta\theta}\right)_{④} \\
\left(T^n_{xy}\right)_{②} = -\left(T^n_{xy}\right)_{①} \\
\left(T^n_{xy}\right)_{③} = -\left(T^n_{xy}\right)_{④} \\
M_{②} = M_{①} \\
M_{③} = M_{④}.
\end{cases}
$$

Similar to paragraph (a) above, the effect of a reflection about the y axis, subject to the conditions (i), is obtained using the following equations for the acceleration of point j,k:

$$
\text{(ii)}\quad \begin{cases}
\phi^n_{j,k} = \frac{1}{4}\left[\left(\rho^0 A^n/V^n\right)_{①} + \left(\rho^0 A^n/V^n\right)_{④}\right] \\
\beta^n_{j,k} = \frac{1}{2}\left\{\left[\left(\Sigma^n_{yy} - \Sigma^n_{\theta\theta}\right)(A^n/M)\right]_{①} + \left[\left(\Sigma^n_{yy} - \Sigma^n_{\theta\theta}\right)(A^n/M)\right]_{④}\right\}.
\end{cases}
$$

$$
\text{(iii)}\quad \left[d\dot{y}/dt\right]_{j,k} = 1/2\phi^n_{j,k}\left\{\left[\left(\Sigma^n_{yy}\right)_{①} - \left(\Sigma^n_{yy}\right)_{④}\right]\left[x^n_{II} - x^n_{III}\right] - \left(T^n_{xy}\right)_{①}\left[y^n_{II} - y^n_{III}\right] - \left(T^n_{xy}\right)_{④}\left[y^n_{I} - y^n_{II}\right]\right\} + \beta^n_{j,k}.
$$

(c) Corner zone on the x axis

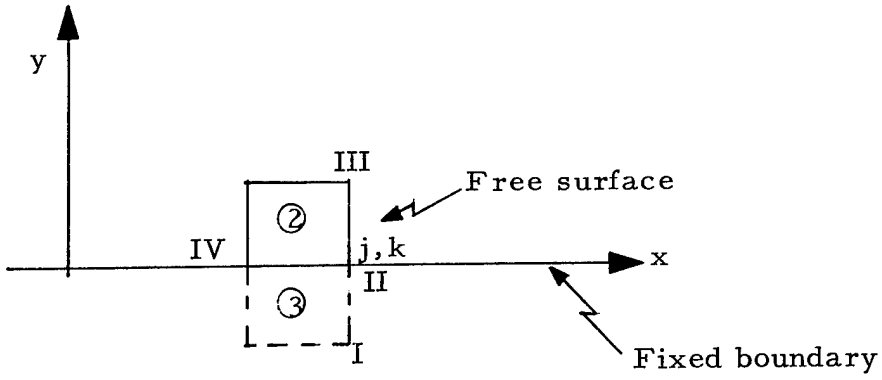

$$\text{(i)}\quad \begin{cases} \dot{y}_{j,k} = 0 \\ \left(\Sigma^n_{xx}\right)_{④} = \left(\Sigma^n_{xx}\right)_{①} = 0 \\ \left(\Sigma^n_{xx}\right)_{③} = \left(\Sigma^n_{xx}\right)_{②} \\ \left(T^n_{xy}\right)_{③} = -\left(T^n_{xy}\right)_{②} \\ \left(T^n_{xy}\right)_{①} = \left(T^n_{xy}\right)_{④} = 0 \\ M_{③} = M_{②}. \end{cases}$$

$$\text{(ii)}\quad \phi_{j,k} = \frac{1}{4}\left[\left(\rho^0 A^n/V^n\right)_{②}\right].$$

$$\text{(iii)}\quad (d\dot{x}/dt)_{j,k} = -\frac{1}{2\phi^n_{j,k}}\left[\left(\Sigma^n_{xx}\right)_{②}\left(y^n_{III} - y^n_{IV}\right) - \left(T_{xy}\right)_{②}\left(x^n_{III} - x^n_{IV}\right)\right].$$

(d) Corner zone on the y axis

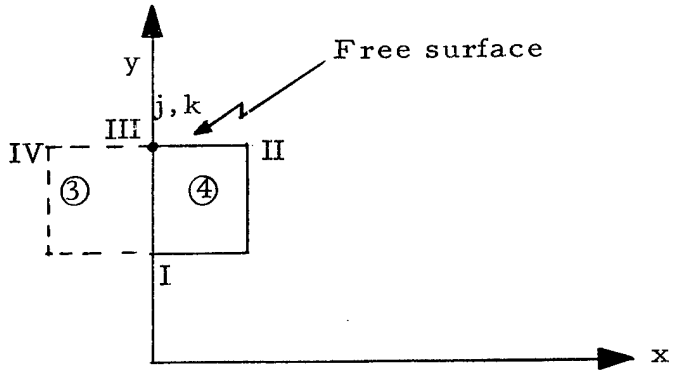

$$\text{(i)}\begin{cases} \dot{x}_{j,k} = 0 \\ \left(\Sigma^n_{yy}\right)_{③} = \left(\Sigma^n_{yy}\right)_{④} \\ \left(\Sigma^n_{yy}\right)_{②} = \left(\Sigma^n_{yy}\right)_{①} = 0 \\ \left(\Sigma^n_{\theta\theta}\right)_{③} = \left(\Sigma^n_{\theta\theta}\right)_{④} \\ \left(\Sigma^n_{\theta\theta}\right)_{②} = \left(\Sigma^n_{\theta\theta}\right)_{①} = 0 \\ \left(T^n_{xy}\right)_{③} = -\left(T^n_{xy}\right)_{④} \\ \left(T^n_{xy}\right)_{②} = \left(T^n_{xy}\right)_{①} = 0 \\ M_{③} = M_{④} \cdot \end{cases}$$

$$\text{(ii)}\begin{cases} \phi^n_{j,k} = \frac{1}{4}\left[\left(\rho^0 A^n/V^n\right)_{④}\right] \\ \beta^n_{j,k} = \left[\left(\Sigma^n_{yy} - \Sigma^n_{\theta\theta}\right)\left(A^n/M\right)\right]_{④} \cdot \end{cases}$$

$$\text{(iii)} \quad \left(d\dot{y}/dt\right)_{j,k} = \frac{1}{2\phi^n_{j,k}}\left[\left(\Sigma^n_{xy}\right)_{④}\left(x^n_I - x^n_{II}\right) - \left(T^n_{xy}\right)_4\left(y^n_I - y^n_{II}\right)\right] + \beta^n_{j,k}$$

(e) Free surfaces

For a free surface at j,k in the figure below, all quantities associated with the phantom zones (1) and (4) are taken as zero. The equations of motion for a general point can then be used, except that $\alpha^n_{j,k}$ and $\beta^n_{j,k}$ are calculated as shown below.

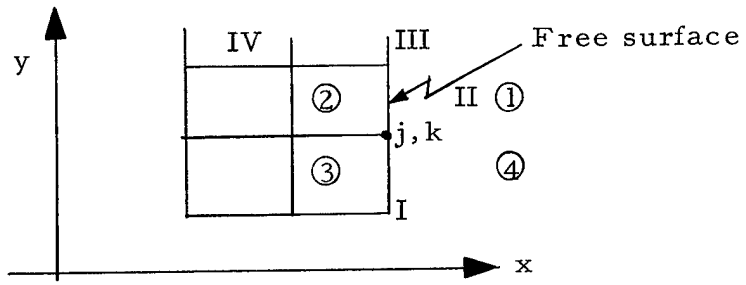

$$\alpha^n_{j,k} = \frac{1}{2}\left\{\left[T^n_{xy}\left(A^n/M\right)\right]_{②} + \left[T^n_{xy}\left(A^n/M\right)\right]_{③}\right\}$$

$$\beta^n_{j,k} = \frac{1}{2}\left\{\left[\left(\Sigma^n_{yy} - \Sigma^n_{\theta\theta}\right)(A^n/M)\right]_{②} + \left[\left(\Sigma^n_{yy} - \Sigma^n_{\theta\theta}\right)(A^n/M)\right]_{③}\right\} .$$

For a corner free surface, the phantom zones in the figures are zones (1), (2), and (4).

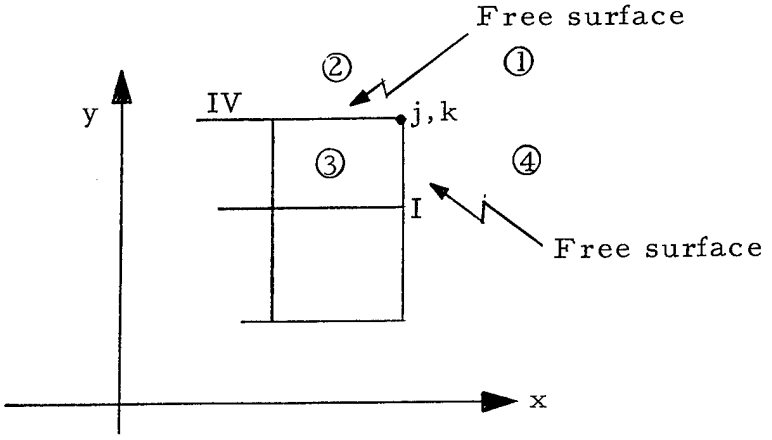

$$\alpha^n_{j,k} = \left(T^n_{xy}\, A^n/M\right)_{③}$$

$$\beta^n_{j,k} = \left[\left(\Sigma^n_{yy} - \Sigma^n_{\theta\theta}\right)\left(A^n/M\right)\right]_{③} .$$

9. Sliding interfaces

When two materials slide on one another, a decoupling of grid points on the interface must be provided, otherwise large grid deformations will result. If all of the forces on the interface are taken into account, the equations of motion become excessively complicated. For a large class of problems a simple decoupling of the grid points gives very satisfactory results. The method adapted here considers one surface to be a fixed boundary during a given time step Δt. The equations of motion for the sliding material are the same as those given for motion along a fixed boundary. The fixed boundary is then advanced in time using the force field of the sliding material next to it. The new position of the fixed boundary provides a new boundary for the sliding material. The important point in this type of calculation is that the parameters on the interface of the sliding material be associated only with the sliding material and that the material providing the fixed boundary be treated as though the boundary were an exterior surface with pressure forces acting on it.

The point is that no forces should be defined at the sliding interface by an averaging process that uses information from either side of the interface.

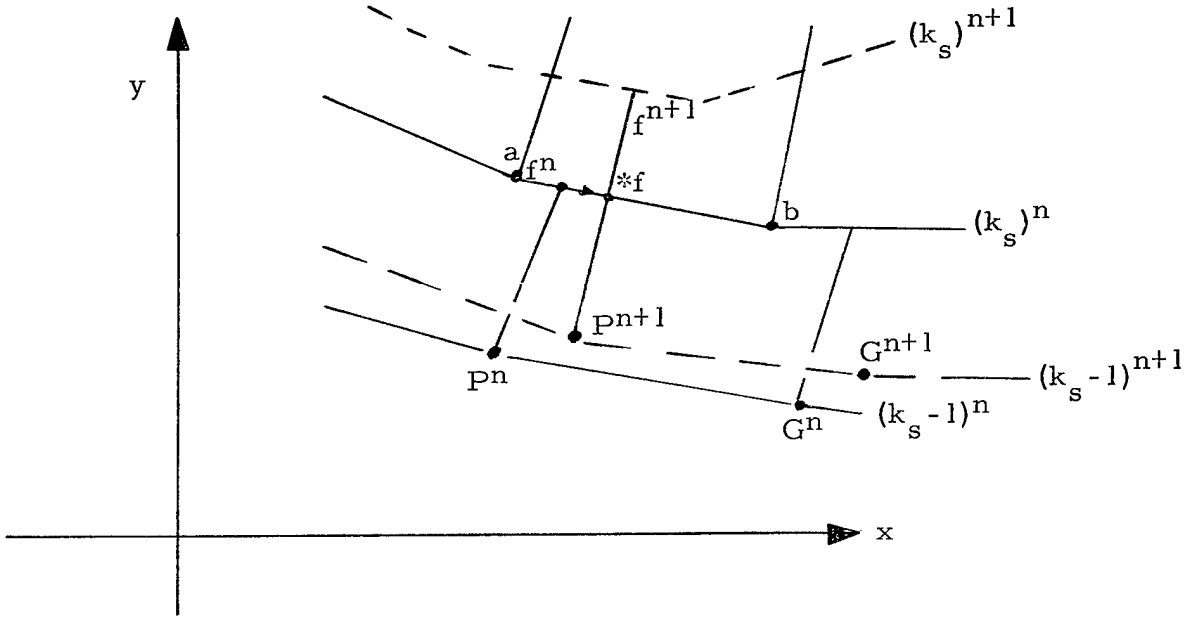

Referring to the figure above:

(1) Point f is advanced along $(k_s)^n$ as though $(k_s)^n$ were a fixed surface. The mass of point f is associated with the mass of the material below k_s.

(2) Points a, b, etc., on $(k_s)^n$ are advanced from time (n) to time (n + 1).

These points are associated with the mass of the grid above k_s. The line $(k_s)^n$ is considered a grid boundary for the material above and accelerated by forces from the grid below.

(3) Points on $(k_s - 1)^n$ are advanced in the usual manner.

(4) The point f^{n+1} if found from the line through P^{n+1} and point *f.

Calculations for a sliding interface

k = slide line

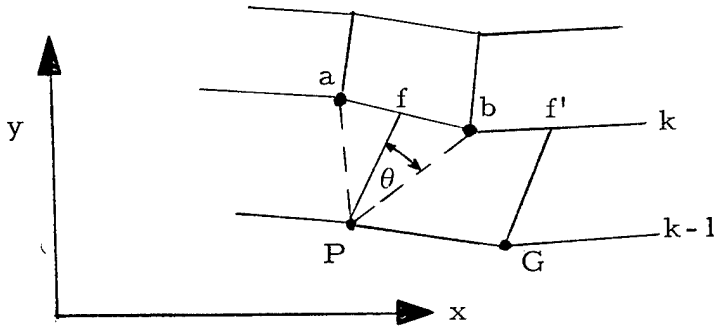

(a) To calculate the volumes of k - 1/2 mass points

1. Given the point P on k - 1 and the slope, m_p, of a line through P; we want to find the points a and b on k that lie to either side of this line (see figure). Once these points are found, the intersection f of a line through points a, b, and the line through P can be determined.

For each point j, k calculate:

$$(\tan\theta)_{j,k} = (m_p - m_{j,k}) \Big/ (1 + m_p \cdot m_{j,k})$$

where:

$$m_{j,k} = (y_{j,k} - y_p) \Big/ (x_{j,k} - x_p)$$

(x_p, y_p) and m_p are given.

(i) If $|m_p| > 10^4$, $(\tan\theta)_{j,k} = 1/m_{j,k}$

(ii) If $|m_{j,k}| > 10^4$, $(\tan\theta)_{j,k} = -1/m_p$

(iii) If $|m_p| > 10^4$ and $|m_{j,k}| > 10^4$, $(\tan\theta)_{j,k} = 0$.

Test the consecutive values of $(\tan\theta)_{j,k}$ until a change in sign is found. The points $(x_{j,k}, y_{j,k})$ and $(x_{j+1,k}, y_{j+1,k})$ where this occurs will be the points (x_a, y_a) and (x_b, y_b). (This method fails if $|\theta| \geq 90°$. However, in practice information on neighboring points is carried from cycle to cycle and these points are tested first. If these fail, points adjoining on either side are alternately tested. For the original search, the whole k line is tested for a change in sign of arctan θ.)

2. To find the coordinates of point f on line ab:

$$x_f = (y_a - y_p + m_p - m_{ab}\, x_a)/(m_p - m_{ab})$$

$$y_f = \{m_p [y_a - m_{ab} (x_a - x_p)] - m_{ab}\, y_p\}/(m_{ab} - m_p)$$

$$m_{ab} = (y_a - y_b)/(x_a - x_b).$$

3. Repeat steps 1 and 2 for point G on k - 1
4. To calculate the volume enclosed by P, f, b, f', and G (see figure).

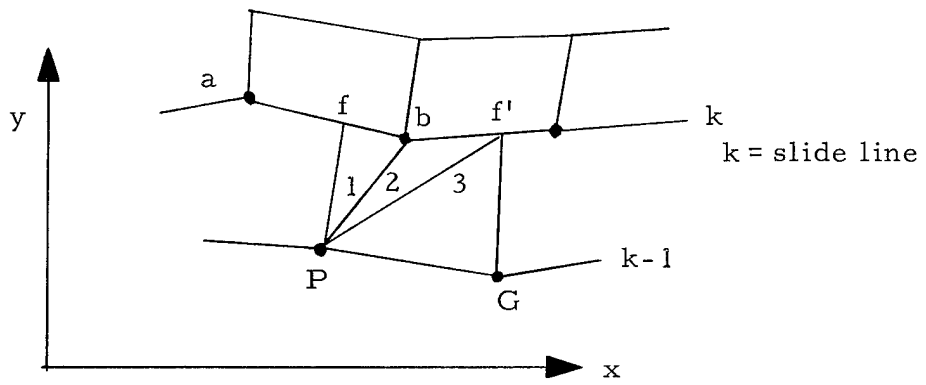

A_1 = area of $\Delta 1$, etc.

$$2A_1 = \begin{vmatrix} i & j & k \\ x_b - x_p & y_b - y_p & 0 \\ x_f - x_p & y_f - y_p & 0 \end{vmatrix} = (x_b - x_p)(y_f - y_p) - (y_b - y_p)(x_f - x_p)$$

$$2A_2 = \begin{vmatrix} i & j & k \\ x_{f'} - x_p & y_{f'} - y_p & 0 \\ x_b - x_p & y_b - y_p & 0 \end{vmatrix} = (x_{f'} - x_p)(y_b - y_p) - (y_{f'} - y_p)(x_b - x_p)$$

$$2A_3 = \begin{vmatrix} i & j & k \\ x_G - x_p & y_G - y_p & 0 \\ x_{f'} - x_p & y_{f'} - y_p & 0 \end{vmatrix} = (x_G - x_p)(y_{f'} - y_p) - (y_G - y_p)(x_{f'} - x_p)$$

$$V_{p+1/2} = \frac{1}{3}\left(\frac{\rho^0}{M}\right)_{p+1/2}\left[(y_p + y_f + y_b)A_1 + (y_p + y_b + y_{f'})A_2 + (y_p + y_{f'} + y_G)A_3\right].$$

5. To calculate the coordinates of the center of a zone

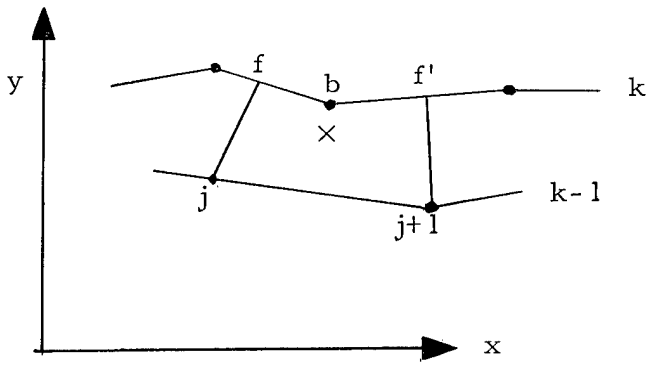

$$x_{j+1/2,k-1/2} = \frac{1}{4}\left(x_{j,k-1} + x_{f,k} + x_{f',k} + x_{j+1,k-1}\right)$$

$$y_{j+1/2,k-1/2} = \frac{1}{4}\left(y_{j,k-1} + y_{f,k} + y_{f',k} + y_{j+1,k-1}\right)$$

(Note: This is not in general the center of a zone, but is suitable for the use that is to be made of it.)

(b) To advance in time point f on the slide line k

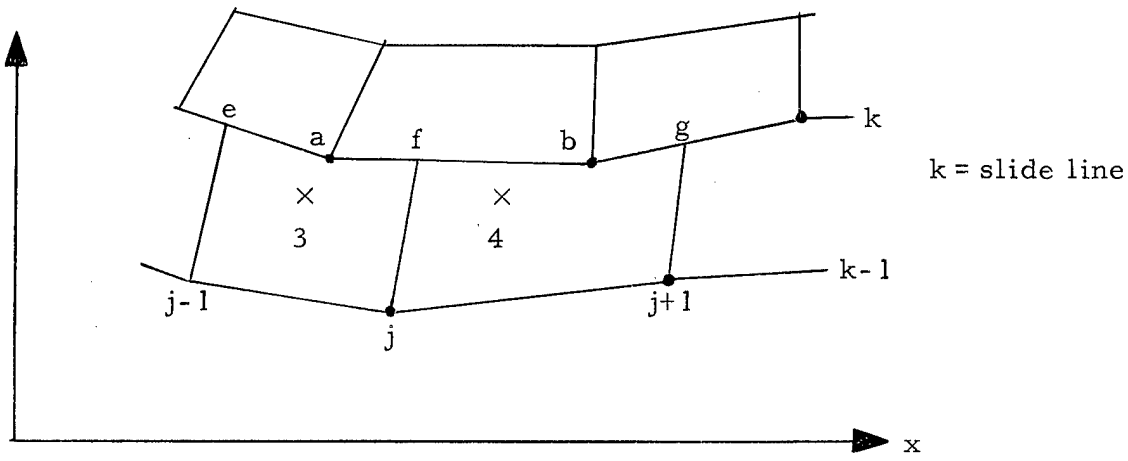

1. $$G_f^n = \left[(P+q)_3\,(y_e - y_{j,k-1}) + (P+q)_4\,(y_{j,k-1} - y_g)\right]^n \cdot \cos \underline{ab}$$
$$- \left[(P+q)_3\,(x_e - x_{j,k-1}) + (P+q)_4\,(x_{j,k-1} - x_e)\right]^n \cdot \sin \underline{ab}.$$

$$\sin \underline{ab} = \left[\frac{y_b - y_a}{\sqrt{(x_b - x_a)^2 + (y_b - y_a)^2}}\right]^n$$

$$\cos \underline{ab} = \left[\frac{x_b - x_a}{\sqrt{(x_b - x_a)^2 + (y_b - y_a)^2}}\right]^n.$$

2. $$\dot{x}_f^{n+1/2} = \dot{x}_{j,k-1}^{n-1/2} + \frac{\Delta t^n}{2\phi_f^n} (G_f \cdot \cos \underline{ab})^n$$

$$\dot{y}_f^{n+1/2} = \dot{y}_{j,k-1}^{n-1/2} - \frac{\Delta t^n}{2\phi_f^n} (G_f \cdot \cos \underline{ab})^n$$

$$\phi_f^n = \frac{1}{4} \left[\left(\frac{\rho^0 A^n}{V^n} \right)_{③} + \left(\frac{\rho^0 A^n}{V^n} \right)_{④} \right].$$

Here $A^n_{③}$ is the area of zone ③ at time n, etc.

Note: The point f at time n-1/2 has been given the velocity of point (j,k-1), also no account is taken of the fact that f may move to a new line segment during a time step.

3. $$x_f^{n+1} = x_f^n + \dot{x}_f^{n+1/2} \Delta t^{n+1/2}$$

$$y_f^{n+1} = y_f^n + \dot{y}_f^{n+1/2} \Delta t^{n+1/2} .$$

(c) To advance in time the point j,k on slide line k

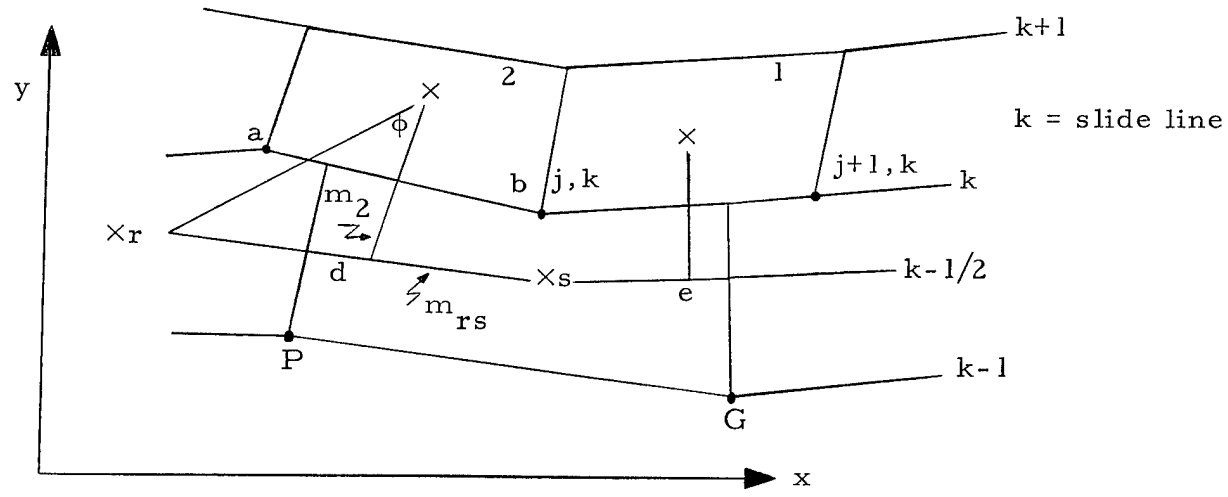

× - center of a zone (see a-5)

1. Given the point 2 in the above figure and the slope m_2 of a line through point 2 and $\perp$ to the face ab. We want to find the points r and s on k - 1/2 that lie to both sides of this line.

For each point (j + 1/2), (k - 1/2) calculate:

$$(\tan\theta)_{j+1/2,k-1/2} = (m_2 - m_{j+1/2,k-1/2})/(1 + m_2 \cdot m_{j+1/2,k-1/2})$$

$$m_{j+1/2,k-1/2} = (y_{j+1/2,k-1/2} - y_2)/(x_{j+1/2,k-1/2} - y_2)$$

$$m_2 = -(x_a - x_b)/(y_a - y_b)$$

(i) If $\left| m_{j+1/2,k-1/2} \right| > 10^4$, $(\tan\theta)_{j+1/2,k-1/2} = -1/m_2$

(ii) If $\left| m_2 \right| > 10^4$, $(\tan\theta)_{j+1/2,k-1/2} \equiv -1/m_{j+1/2,k-1/2}$

(iii) If $\left| m_2 \right| > 10^5$ and $\left| m_{j+1/2,k-1/2} \right| > 10^5$, $(\tan\theta)_{j+1/2,k-1/2} = 0$.

Test consecutive values of $(\tan\theta)_{j+1/2,k-1/2}$ until a change in sign is found. The points $(x_{j-1/2,k-1/2}, y_{j-1/2,k-1/2})$ and $(x_{j+1/2,k-1/2}, y_{j+1/2,k-1/2})$ will be the points (x_r, y_r) and (x_s, y_s) (see details in Part I).

2. Calculate the point of intersection (x_d, y_d) of the line through Point 2 and the line through points (x_r, y_r) and (x_s, y_s).

$$x_d = (m_{rs}x_r - m_2x_2 + y_2 - y_r)/(m_{rs} - m_2)$$

$$y_d = \left\{m_2\left[y_r - m_{rs}(x_r - x_2)\right] - m_{rs}y_2\right\}/(m_2 - m_{rs})$$

$$m_{rs} = (y_r - y_s)/(x_r - x_s)$$

If $\left| m_{rs} \right| < 10^{-4}$, and $\left| m_2 \right| > 10^4$, $x_d = x_2$ and $y_d = y_s$.

3. Calculate the pressure at point d

$$P_d = P_r \left| d - s \right| + P_s \left| d - r \right| / \left| r - s \right|$$

$$\left| d - s \right| = \sqrt{(x_d - x_s)^2 + (y_d - y_s)^2}\ , \text{ etc.}$$

4. Repeat 1 through 3 to get P_e
5. Advance point (j,k)

$$\dot{x}^{n+1/2}_{j,k} = \dot{x}^{n-1/2}_{j,k} + \frac{\Delta t^n}{2\phi^n_{j,k}} \left\{ \begin{array}{l} P^n_1\left(y^n_{j+1,k} - y^n_{j,k+1}\right) + P^n_2\left(y^n_{j,k+1} - y^n_{j-1,k}\right) \\ + P_d\left(y^n_{j-1,k} - y^n_{j,k}\right) + P_e\left(y^n_{j,k} - y^n_{j+1,k}\right) \end{array} \right\}$$

$$\dot{y}^{n+1/2}_{j,k} = \dot{y}^{n-1/2}_{j,k} - \frac{\Delta t^n}{2\phi^n_{j,k}} \left\{ \begin{array}{l} P^n_1\left(x^n_{j+1,k} - x^n_{j,k+1}\right) + P^n_2\left(x^n_{j,k+1} - x^n_{j-1,k}\right) \\ P^n_d\left(x^n_{j-1,k} - x^n_{j,k}\right) + P^n_e\left(x^n_{j,k} - x^n_{j+1,k}\right) \end{array} \right\}.$$

(d) The rest of the grid is advanced with the normal equations. The slope m_p of Section I is found from (x_f, y_f) of Section II and the advanced position of point P. We are now ready to repeat steps (a) through (b). The original slope m_p is obtained by bisecting the angle made by point P and its neighboring points on line $(k_s - 1)$.

(e) Discussion:

From the above procedure it is seen that the sliding material is made to follow the motion of the slide line boundary. An error in time and position is introduced since, even though mass is conserved, one-half the mass of the sliding material is not used in the calculation of the acceleration in the direction of the boundary motion. This error is reduced when the sliding material has a smaller density than the material associated with the boundary or when small grid zones are used. For reasonable zoning, the error only shows up after large displacements have taken place. The error can be effectively remedied by increasing the mass in the boundary material to compensate for the one-half mass in the sliding material that has been neglected in the acceleration equations.

10. High-explosive burn options

The chemical energy to be released through the hydrodynamic equation of state is stored in each high-explosive zone as an initial energy E^0. The time for the detonation front to reach a specific zone is calculated in advance from the known detonation velocity, D, and the distance from the point of detonation to the center of the zone. This quantity is also stored with each zone. A Burn fraction, F, is calculated so as to spread the burn front over several zones analogous to the artificial viscosity "q" that spreads a shock over several zones. The burn fraction is integrated with the energy equation and the explicit form shown in Section 5 for calculating the energy cannot be used. Instead, the energy must be calculated by an iteration procedure. The procedure given below can also be used to replace the calculation shown in Section 5 when a more complicated equations of state is required.

For one-dimensional calculations the burn fraction can be defined as $F = (1-V)/(V_{CJ})$ (Ref. 11) and the burn calculation is started by setting $F = 1$ in the zone that corresponds to the point of detonation. The burn calculation will proceed to around three or four times the number of zones that the artificial viscosity "q" is spread over before the detonation front is correctly established. For one-dimensional calculations this amounts to about 16 zones. In two-dimensional calculations where there is a limit to the number of zones for a practical problem, it is usually necessary to have the correct detonation velocity established in a fewer number of zones. A convenient way to do this is to start the burn calculation at the time the detonation would reach a given zone as described above. To allow for the possibility of an overdriven detonation that may arise during the calculation and result in a higher than normal detonation velocity, the burn fraction $F = (1-V)/(1-V_{CJ})$ can be used in addition to the burn fraction that is based on the known detonation velocity. The larger of the two is then selected for the calculation.

(i) Burn fraction = $F_1^{n+1} = (t^{n+1} - t_b)/\Delta L$

For $t^{n+1} \leq t_b$: $F_1^{n+1} = 0$

$F_2^{n+1} = (1-V^{n+1})/(1-V_{CJ})$

F^{n+1} = maximum of F_1^{n+1} and F_2^{n+1}

If $F^{n+1} > 1$ set $F^{n+1} = 1$

$\Delta L = r\Delta x/D$

t = actual time

t_b = time for a zone to start burning

Δx = grid spacing

D = detonation velocity

r = constant ≈ 2.5

V_{CJ} = Chapman-Jouguet relative volume

(ii) $\tilde{E}^{n+1} = E^n - (P^n + q^{n+1/2}) \cdot (V^{n+1} - V^n)$.

(iii) $\tilde{P}^{n+1} = P(\tilde{E}^{n+1}, V^{n+1}) \cdot F^{n+1}$,

here $P(E, V)$ is the equation of state of the burned explosive.

(iv) $E^{n+1} = \tilde{E}^{n+1} - 1/2(\tilde{P}^{n+1} - P^n) \cdot (V^{n+1} - V^n)$.

(v) $P^{n+1} = P(E^{n+1}, V^{n+1}) \cdot F^{n+1}$.

11. Stability

The Δt calculation is the same as that given for the one-dimensional problem in Appendix A. The characteristic zone thickness is taken to be the zone area divided by the longest diagonal.

12. Plane geometry

For plane geometry in x-y space, the mass calculation corresponding to Eq. (1a) at the beginning of the appendix becomes:

$$M_{①} = \rho^0/V_0 (A_a^0 + A_b^0).$$

The conservation of mass Eq. (2) becomes:

$$V_{①}^n = \left(\rho^0/M_{①}\right) \cdot \left(A_a^n + A_b^n\right).$$

In the equations of motion [Eq. (3)] the terms α and β are set to zero. The quantity $\phi_{j,k}$ is seen to be a constant and is calculated only once for each point j,k. The logic for the value of $\phi_{j,k}$ at grid boundaries is the same as for the cylindrical case where $[\rho_0(A_b^n + A_b^n)/V^n]_{①} = M_{①}$, etc.

The term $\dot{\epsilon}_{\theta\theta}$ in the equation of state section is set to zero.